



Norwegian University of  
Science and Technology

# Aerodynamic Development and Construction of a Car for Participation in the Eco-Marathon Competition

**Morten Stenstad Lien**

Master of Science in Product Design and Manufacturing

Submission date: June 2010

Supervisor: Lars Sætran, EPT





# Problem Description

## Bakgrunn

Shell Eco-Marathon er en konkurranse mellom studentgrupper om å utvikle, bygge og kjøre den mest energigjerrige bilen. Konkurransen går årlig i Europa i mai, og den har nå gått i 24 år. NTNUs første deltakelse i 2008 var en stor suksess, og laget endte opp med en andreplass. I 2008/09 arbeidet en tverrfaglig gruppe på 10 studenter med en Urban Concept-bil som prosjekt- og masteroppgave. Resultatet ble DNV Fuel Fighter, en bil på 70 kg, drevet av en elektrisk mo-tor og en brenselcelle som omdanner hydrogen til elektrisitet. 9. mai 2009 knuste laget fra NTNU alle 200 motstanderlag, og satte verdensrekord hvor Fuel Fighter klarte å legge bak seg hele 1246 km på energi tilsvarende en liter bensin.

Det er etablert en prosjektgruppe med ansvar for å utvikle og lage bilen for 2010. Prosjektet er et samarbeidsprosjekt mellom et antall studenter fra flere ulike fagmiljø ved NTNU, og det forutsetter også sponsorarbeid, arbeidet med de dokumentene som er nødvendige for å melde på bilen til konkurransen samt organisering og gjennomføring av selve løpet våren 2010.

## Mål

Den eksisterende bilen (se ovenfor) skal gjøres bedre, og aerodynamisk motstand er identifisert som en viktig faktor i så måte. Oppgaven vil være å drive et testprogram på bilen i instituttets vindtunnel samt utarbeide og produsere løsninger for å forebedre den aerodynamiske ytelsen til bilen.

Arbeidet i prosjektoppgaven foregår på fire nivå:

- Prosjektet i sin helhet inklusive offentlighetsarbeid, prosjektstyring og sponsorarbeid

- Selve bilen som et samspill av alle sine enkeltsystemer

- Enkeltsystemene med tilhørende interface

- Nødvendige eksterne tekniske og organisatoriske støttesystemer knyttet til bygging, testing og gjennomføring

Arbeidet skal utføres i samarbeid med prosjektgruppen. Kandidaten må bidra på tvers av alle 4 nivå og samtidig ta et helhetlig ansvar for definerte deloppgaver som defineres i prosjektplanen. Arbeidet bedømmes både med hensyn til helheten og med hensyn til kandidatens deloppgaver. Bedømmelsen tar hensyn til både sluttresultatene og dokumentasjonen i utviklingsarbeidet. Besvarelsen skal i hovedsak behandle det aerodynamiske aspektet ved prosjektet, men også det produksjonsmessige skal dokumenteres.

Assignment given: 18. January 2010

Supervisor: Lars Sætran, EPT





## MASTEROPPGAVE

for

Stud.techn. Henrik Aaserud Eikeland og Stud.techn. Morten Stenstad Lien

Våren 2010

### AERODYNAMISK UTVIKLING OG BYGGING AV BIL FOR DELTAKELSE I SHELL ECO-MARATHON-KONKURRANSEN

#### Aerodynamic development and construction of a car for participation in the Eco-Marathon competition

#### Bakgrunn

Shell Eco-Marathon er en konkurranse mellom studentgrupper om å utvikle, bygge og kjøre den mest energigjerrige bilen. Konkurransen går årlig i Europa i mai, og den har nå gått i 24 år. NTNUs første deltakelse i 2008 var en stor suksess, og laget endte opp med en andreplass. I 2008/09 arbeidet en tverrfaglig gruppe på 10 studenter med en Urban Concept-bil som prosjekt- og masteroppgave. Resultatet ble DNV Fuel Fighter, en bil på 70 kg, drevet av en elektrisk motor og en brenselcelle som omdanner hydrogen til elektrisitet. 9. mai 2009 knuste laget fra NTNU alle 200 motstanderlag, og satte verdensrekord hvor Fuel Fighter klarte å legge bak seg hele 1246 km på energi tilsvarende en liter bensin.

Det er etablert en prosjektgruppe med ansvar for å utvikle og lage bilen for 2010. Prosjektet er et samarbeidsprosjekt mellom et antall studenter fra flere ulike fagmiljø ved NTNU, og det forutsetter også sponsorarbeid, arbeidet med de dokumentene som er nødvendige for å melde på bilen til konkurransen samt organisering og gjennomføring av selve løpet våren 2010.

#### Mål

Den eksisterende bilen (se ovenfor) skal gjøres bedre, og aerodynamisk motstand er identifisert som en viktig faktor i så måte. Oppgaven vil være å drive et testprogram på bilen i instituttets vindtunnel samt utarbeide og produsere løsninger for å forebedre den aerodynamiske ytelsen til bilen.

Arbeidet i prosjektoppgaven foregår på fire nivå:

- Prosjektet i sin helhet inklusive offentlighetsarbeid, prosjektstyring og sponsorarbeid
- Selve bilen som et samspill av alle sine enkeltsystemer
- Enkeltsystemene med tilhørende interface
- Nødvendige eksterne tekniske og organisatoriske støttesystemer knyttet til bygging, testing og gjennomføring



Arbeidet skal utføres i samarbeid med prosjektgruppen. Kandidaten må bidra på tvers av alle 4 nivå og samtidig ta et helhetlig ansvar for definerte deloppgaver som defineres i prosjektplanen. Arbeidet bedømmes både med hensyn til helheten og med hensyn til kandidatens deloppgaver. Bedømmelsen tar hensyn til både sluttresultatene og dokumentasjonen i utviklingsarbeidet. Besvarelsen skal i hovedsak behandle det aerodynamiske aspektet ved prosjektet, men også det produksjonsmessige skal dokumenteres.

” - ”

Senest 14 dager etter utlevering av oppgaven skal kandidaten levere/sende instituttet en detaljert fremdrift- og eventuelt forsøksplan for oppgaven til evaluering og eventuelt diskusjon med faglig ansvarlig/veiledere. Detaljer ved eventuell utførelse av dataprogrammer skal avtales nærmere i samråd med faglig ansvarlig.

Besvarelsen redigeres mest mulig som en forskningsrapport med et sammendrag både på norsk og engelsk, konklusjon, litteraturliste, innholdsfortegnelse etc. Ved utarbeidelsen av teksten skal kandidaten legge vekt på å gjøre teksten oversiktlig og velskrevet. Med henblikk på lesning av besvarelsen er det viktig at de nødvendige henvisninger for korresponderende steder i tekst, tabeller og figurer anføres på begge steder. Ved bedømmelsen legges det stor vekt på at resultatene er grundig bearbeidet, at de oppstilles tabellarisk og/eller grafisk på en oversiktlig måte, og at de er diskutert utførlig.

Alle benyttede kilder, også muntlige opplysninger, skal oppgis på fullstendig måte. For tidsskrifter og bøker oppgis forfatter, tittel, årgang, sidetall og eventuelt figurnummer.

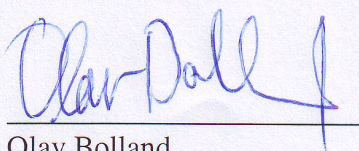
Det forutsettes at kandidaten tar initiativ til og holder nødvendig kontakt med faglærer og veileder(e). Kandidaten skal rette seg etter de reglementer og retningslinjer som gjelder ved alle (andre) fagmiljøer som kandidaten har kontakt med gjennom sin utførelse av oppgaven, samt etter eventuelle pålegg fra Institutt for energi- og prosesssteknikk.

I henhold til ”Utfyllende regler til studieforskriften for teknologistudiet/sivilingeniørstudiet” ved NTNU § 20, forbeholder instituttet seg retten til å benytte alle resultater og data til undervisnings- og forskningsformål, samt til fremtidige publikasjoner.

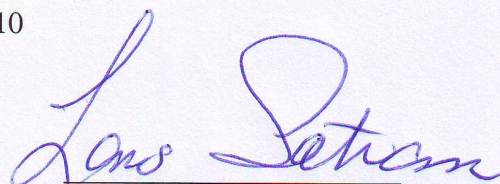
Ett -1 komplett eksemplar av originalbesvarelsen av oppgaven skal innleveres til samme adressat som den ble utlevert fra. Det skal medfølge et konsentrert sammendrag på maksimalt én maskinskrevet side med dobbel linjeavstand med forfatternavn og oppgavetittel for evt. referering i tidsskrifter).

Til Instituttet innleveres to - 2 komplette kopier av besvarelsen. Ytterligere kopier til eventuelle medveiledere/oppgavegivere skal avtales med, og eventuelt leveres direkte til de respektive. Til instituttet innleveres også en komplett kopi (inkl. konsentrerte sammendrag) på CD-ROM i Word-format eller tilsvarende.

NTNU, Institutt for energi- og prosesssteknikk, 12. januar 2010



Olav Bolland  
Instituttleder



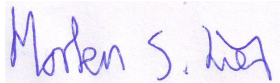
Lars Sætran  
Faglig ansvarlig/veileder



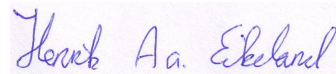
## Acknowledgements

We would like to take this opportunity to thank the whole DNV Fuel Fighter team for a fantastic experience, as well as our supervisor professor Lars Sætran, technical personnel, Kristina Dahlberg from our main sponsor DNV, suppliers and fellow students who have contributed to the project with time, knowledge and resources.

A special thanks is directed to Lars Øien at SINTEF Marine who managed to mill the end extension mould on very short notice and at his own personal inconvenience. Also thanks to the people at Thermal Energy Group at Department of Energy and Process Engineering for their kind assistance with the oven for the carbon fiber curing process.



Morten Stenstad Lien



Henrik Aaserud Eikeland



### **Abstract**

The authors of this paper were responsible for aerodynamic development of, as well as assisting in the production of components for, the NTNU vehicle for the Shell Eco-marathon competition, DNV Fuel Fighter. A drag reducing end extension, with the intent of delaying flow separation, was designed, produced and mounted on the vehicle. Due to wind tunnel breakdown the final product could not be tested, but the prototype was measured to give a drag reduction of between 8% and 15% for  $0^\circ$  to  $15^\circ$  yaw angle. During the competition the team did not complete an approved run due to technical difficulties with the propulsion and the electronic control system.





## **Sammendrag**

Forfatterne av denne oppgaven var ansvarlige for den aerodynamiske utviklingen av, så vel som å støtte i produksjonen av diverse komponenter for, NTNU sin bil for Shell Eco-maraton konkurransen, DNV Fuel Fighter. En forlengelse til bilen med den hensikt å utsette separasjon av strømmingen og dermed redusere luftmotstand, ble designet, produsert og montert på bilen. Dessverre kunne ikke sluttproduktet testes på grunnnet sammenbrudd av vindtunnelen. Prototypen av forlengelsen ble målt til å gi en reduksjon av luftmotstand på mellom 8% og 15% for  $0^\circ$  til  $15^\circ$  innstrømningsvinkel. Under konkurransen gjennomførte ikke laget et godkjent løp grunnnet tekniske problemer med fremdrifts- og styresystemet.



# Contents

<b>1</b>	<b>Introduction</b>	<b>1</b>
1.1	Statement of Problem . . . . .	1
1.2	About Shell Eco-marathon . . . . .	1
1.3	The DNV Fuel Fighter 2010 team . . . . .	2
1.4	Background Information . . . . .	2
<b>2</b>	<b>Literature on Car Aerodynamics</b>	<b>6</b>
2.1	Aerodynamic Drag . . . . .	6
2.2	Coefficients of Drag . . . . .	9
2.3	Vehicles in Cross-winds . . . . .	10
2.4	Diffuser and Ground Clearance . . . . .	11
2.5	Implications of Theory . . . . .	12
<b>3</b>	<b>Test Methods</b>	<b>13</b>
3.1	CFD . . . . .	13
3.2	Wind Tunnel Testing . . . . .	14
3.2.1	Blockage . . . . .	14
3.2.2	Small Scale Testing and Reynolds Effects . . . . .	15
3.2.3	The Moving Road Problem . . . . .	17
3.2.4	Visualization . . . . .	18
3.3	CFD and Wind Tunnel Testing in This Project . . . . .	18
<b>4</b>	<b>Presentation of Work</b>	<b>20</b>
4.1	Areas of Improvement . . . . .	20
4.1.1	Surface Friction . . . . .	20
4.1.2	Protuberance Drag . . . . .	21
4.1.3	Driver Ventilation . . . . .	22
4.1.4	Fuel Cell Ventilation . . . . .	23
4.2	Experimental Setup . . . . .	24
4.3	Experimental Equipment . . . . .	25

4.3.1	Wind Tunnel . . . . .	25
4.3.2	Pitot . . . . .	25
4.3.3	Scale . . . . .	28
4.3.4	Labview - Forcelog . . . . .	29
4.3.5	Amplifiers . . . . .	29
4.4	Test Procedure . . . . .	29
4.5	Wind Tunnel Testing . . . . .	30
4.5.1	Extension Prototype . . . . .	32
4.6	Calculation Inputs . . . . .	32
4.6.1	Projected Frontal Area . . . . .	33
4.7	Results . . . . .	34
4.7.1	Blockage and $C_d$ -value . . . . .	36
4.7.2	Discussion of Error Sources . . . . .	38
4.8	Computer Aided Design . . . . .	39
4.9	Production . . . . .	40
4.9.1	Production at Kongsberg . . . . .	40
4.9.2	Milling of Mould . . . . .	41
4.9.3	Carbon Fiber Moulding . . . . .	41
4.9.4	Curing Process . . . . .	42
4.9.5	Materials . . . . .	43
4.9.6	Production Problems . . . . .	44
4.10	Final Design . . . . .	46
<b>5</b>	<b>Conclusion</b> . . . . .	<b>48</b>
5.1	Notes on Shell Eco-marathon 2010 . . . . .	48
5.2	Conclusion . . . . .	48

# List of Figures

1.1	DNV Fuel Fighter 2010 . . . . .	3
1.2	Previous versions . . . . .	4
1.3	PAC-Car II . . . . .	5
2.1	Pillar positions. . . . .	7
2.2	Skin-friction coefficient $C_f$ values on a flat plate. . . . .	8
2.3	Generation of strong conical vortices around the D-pillar. . . . .	8
2.4	Effect of rear body slope on afterbody drag. . . . .	9
2.5	Coordinate system. . . . .	10
3.1	Blockage diagram . . . . .	16
3.2	Moving belt . . . . .	18
3.3	Reversed Flow . . . . .	19
4.1	3D model of front wheel covers. . . . .	22
4.2	Fuel cell with ventilation tubes in gray. . . . .	24
4.3	Wind tunnel test setup. . . . .	25
4.4	Pitot calibration setup schematic. . . . .	26
4.5	Pitot calibration constant. . . . .	27
4.6	Rolling resistance and aerodynamic drag with speed. . . . .	28
4.7	Rig placement wind tunnel test 1 . . . . .	31
4.8	Results wind tunnel test 2 . . . . .	31
4.9	Prototype model mounted on car . . . . .	32
4.10	Projected area . . . . .	34
4.11	Comparison PureChoice-configuration . . . . .	35
4.12	Results wind tunnel test 06.03.2010 . . . . .	35
4.13	Extension prototype 2009 . . . . .	36
4.14	Comparison of correction methods . . . . .	37
4.15	$C_d$ comparison different speeds . . . . .	39
4.16	Exploded view of DNV Fuel Fighter 2010. . . . .	40
4.17	End extension moulds. . . . .	42

4.18	Provisional oven. . . . .	43
4.19	Mould with initial bag solution. . . . .	45
4.20	Finished casted end extension. . . . .	45
4.21	Points of velocity measurements. . . . .	46
5.1	DNV Fuel Fighter 2010. . . . .	49

# List of Tables

- 1.1 Team members . . . . . 2
- 4.1 Input Data . . . . . 33
- 4.2 Improvement drag prototype . . . . . 36
- 4.3 Measured velocities along car body. . . . . 46





# Chapter 1

## Introduction

### 1.1 Statement of Problem

In the context of improving the existing Shell Eco-marathon vehicle from NTNU, aerodynamics have been identified as a substantial element in the potential for improvement. The assignment will consist of running a test program in Department of Energy and Process Engineering's wind tunnel, as well as development and production of solutions improving the aerodynamic performance of the vehicle.

Additionally, work on various aspects of the vehicle development and project management as a whole is required. This includes assisting in the machining, construction and assembly of components for the vehicle, as well as miscellaneous administrative tasks.

### 1.2 About Shell Eco-marathon

Shell Eco-Marathon is a student competition where the challenge is to design and build a car that can drive as far as possible on an energy quantity equal to 1 l of gasoline. Shell Eco-Marathon was introduced in 1939 as an internal wager between Shell scientists in Wood River, Illinois, USA, but was first arranged in its current form in France in 1985 [1]. The teams can compete in two different categories; Prototypes and UrbanConcept. The Prototype class has few restrictions on design and the cars can be built with emphasis on efficiency and drag reduction, while the UrbanConcept class are to a certain extent regulated to appear more like conventional passenger cars. NTNU participated for the first time in 2008 under

the name "PureChoice", where they came second in the UrbanConcept class. In 2009, NTNU beat the world record driving 1246 km/l [2] under the name "DNV Fuel Fighter". Since 2009, the Shell Eco-marathon has been arranged at the Eurospeedway Lausitz, Germany. The goal this year, decided by the team during fall project, was to improve the world record from last year and drive 1500 km/l.

### 1.3 The DNV Fuel Fighter 2010 team

The multidisciplinary team this year consists of 13 students from five different departments, as given in table 1.1 and depicted in figure 1.1. The four students from Product Development and Materials started in September with planning, mapping of feasible car improvements, recruitment of team members and getting sponsors as a part of their fall project.

Students	Field of study	Areas of responsibility
Åsmund Bekkevold	Product Development and Materials	Team leader
Magnus Storsveen, Ståle F. Antonsen, Nicolai I. Stubbrud	Product Development and Materials	New wheel suspension, dashboard, brakes, door, wheel rims
Henrik Aa. Eikeland, Morten S. Lien	Energy and Process Engineering	Aerodynamics, logistics
Torstein Skarsgard	Chemical Engineering	Improvement of fuel cell
André Dahl-Jacobsen	Electric Power Engineering	New electric motor
Anders Guldahl	Engineering Cybernetics	Improvement of the electric control system
Silje L. Owrenn, Hanne Strypet, Elise F. Myrtrøen	Social Science and Technology Management	PR and media
Lorenz Baur	Exchange student from Germany	Ventilation of fuel cell

Table 1.1: Team members with their respective areas of responsibility.

### 1.4 Background Information

As mentioned earlier, the car has been used in the Shell Eco-marathon competition two times before. The PureChoice-team built the car in 2008 as shown in



Figure 1.1: The DNV Fuel Fighter team 2010. Photo: Trine Ørndahl og Kari Grimsbø.

figure 1.2(a). The CFD-program ANSYS Fluent was used in the design process to optimize the car aerodynamics. The duct underneath the car was implemented for structural strength and to reduce the frontal area of the car, and hence reduce drag [3]. The Fluent analysis showed that the flow above the car remained attached until the back end of the car. Therefore, their report suggested to extend the lines of the top and bottom part of the car into a point, to reduce the separation zone. The 2009 DNV Fuel Fighter team solved this with an extension as seen in figure 1.2(b). The team also made new mirrors which were placed inside the driver compartment, and hence eliminated the drag contribution from external mirrors. A third change was the closure of the duct underneath the car. The argumentation for this decision was that they were not sure whether the tunnel had a positive contribution to drag reduction or not [4]. The effect of these changes will be discussed later.



(a) PureChoice - 2008



(b) DNV Fuel Fighter - 2009

Figure 1.2: The two previous versions of the car. Figures in courtesy of the PureChoice team 2008 and the DNV Fuel Fighter team 2009, respectively.

The Shell Eco-marathon rules [5] set a number of constraints for the design in the UrbanConcept class, some of which may directly limit the aerodynamic optimization. While most of the vehicles in the Prototype class are long, sleek and have very low frontal area like the PAC-Car II vehicle shown in figure 1.3, the UrbanConcept vehicles are bounded by the following dimensions:

- Height: 100 – 130 cm
- Width: 120 – 130 cm
- Length: 220 – 350 cm

In addition, the ground clearance needs to be at least 10 cm, a suitcase-like object of size  $50 \times 40 \times 20$  cm must be placed in the compulsory luggage compartment, and the vehicle needs exactly four wheels. The door opening mechanism must be

accessible from both the inside and outside, and the door cannot be sealed with adhesive tape. The radius of sharp points must be larger than 5 cm or be made of foam or similar deformable material, and aerodynamic appendages in which can be adjusted while driving are not allowed.



Figure 1.3: PAC-Car II, the world's most fuel efficient vehicle [6]. Picture courtesy of ETH [7].

## Chapter 2

# Literature on Car Aerodynamics

Development of a vehicle for the Shell Eco-marathon competition is quite different from that of a conventional road vehicle. With the required minimum average speed of 25 km/h and the single goal of minimizing fuel consumption, many elements of the literature concerning car aerodynamics were found to be irrelevant. The following is a brief summary of the theory that was considered applicable to the aerodynamic development of this particular vehicle.

### 2.1 Aerodynamic Drag

Aerodynamic drag will be defined as the axial or longitudinal force resulting from air flowing past the vehicle body. The two components, pressure drag and skin friction, account for the aerodynamic drag of a vehicle in its entirety. Estimating the relative magnitudes of the two components would give, very approximately, a value of 10% from skin friction and the remaining 90% from pressure drag. An alternative representation of the drag is as the momentum loss of the air in the vehicle wake, along with the rotational energy imparted to this air by vorticity generated by the vehicle [8].

If desired, the drag can be divided into components related to the various regions and parts of the vehicle; forebody and afterbody pressure drag, underbody drag, protuberance drag and the skin friction on the upper body surface. Afterbody pressure drag is dictated by the extent to which pressure can be recovered at the rear of the vehicle body. The "base pressure", with base being the surface in contact with the wake, may be manipulated by altering its geometry [8].

The two main contributors to protuberance drag is the drag of wheels and wheel

wells. Simple estimations and measurements give rough estimates on the magnitude of these contributions. Carr G.W. [8] estimate these to be 0,015 – 0,060 and 0,035 contribution to  $C_d$  for the wheels and wheel wells, respectively. Methods for reducing drag contributions by wheels and wheel wells are enclosure of the wheels, flush wheel discs, and shaping of the body around the wheel wells such that minimal flow disturbance is obtained. On conventional road vehicles there will also be a protuberance drag contribution from drip rails along the A-pillars and D-pillars (see figure 2.1) as well as from externally mounted mirrors [8]. The profile of the

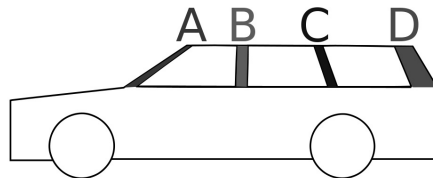


Figure 2.1: The positions of the four pillars on a conventional road vehicle.

trailing edge distinctly influences the drag of the vehicle. A rounded edge may form a suction peak due to the flow tending to follow the curve, resulting in higher drag. Lower drag, however, may result from a square edge [8].

The boundary layer thickness on the surface of a vehicle will decrease as airspeed increases. This effect is due to the larger momentum of the free stream compared to the loss of momentum caused by the viscosity near the solid surface. As a result of this, the friction coefficient will be reduced with increased Reynolds number, as seen in figure 2.2. This applies in laminar as well as turbulent flows, but the extent to which this reduces drag will differ between the two [9].

Conical vortices tend to form around the D-pillar (see figure 2.1) at the rear of road vehicles creating a region of low pressure, as illustrated in figure 2.3. These vortices affect the boundary layer from the rear screen such that attached flow can be maintained on the rear screen even at rake angles as high as  $30^\circ$ . This would seem beneficiary with respect to drag, but this is not necessarily the case. The problem is that by pulling the air downwards maintaining attached flow, the change in flow momentum creates forces on the car which has both drag and lift components [10].

As seen in figure 2.4, increasing the slope will initially reduce the drag, but when the rake angle ( $\theta$  in figure 2.4) exceeds approximately  $10^\circ$  the aforementioned strong conical vortices will start to form and drag increases. Experimental results indicate that the peak drag is at approximately  $30^\circ$ . Higher rake angles than this will prevent stable vortices from forming due to separation, with drag dropping to a relatively fixed value for the remainder of rake angles up to  $90^\circ$  [10].

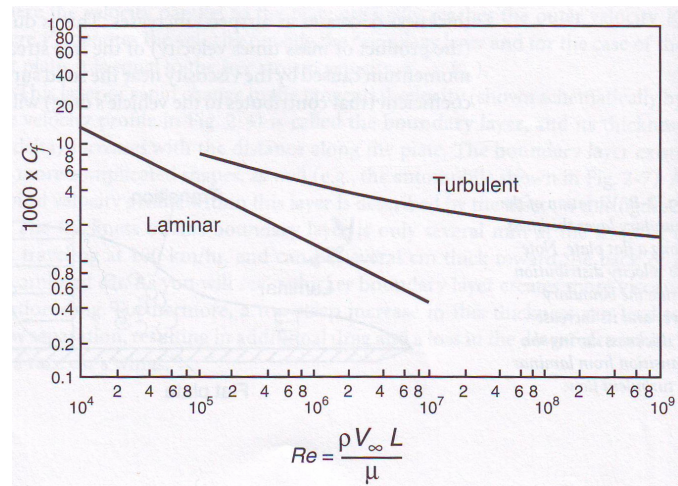


Figure 2.2: Skin-friction coefficient  $C_f$  values on a flat plate, placed parallel to the flow, for laminar and turbulent boundary layers, versus the Reynolds number. Figure by Katz [9].

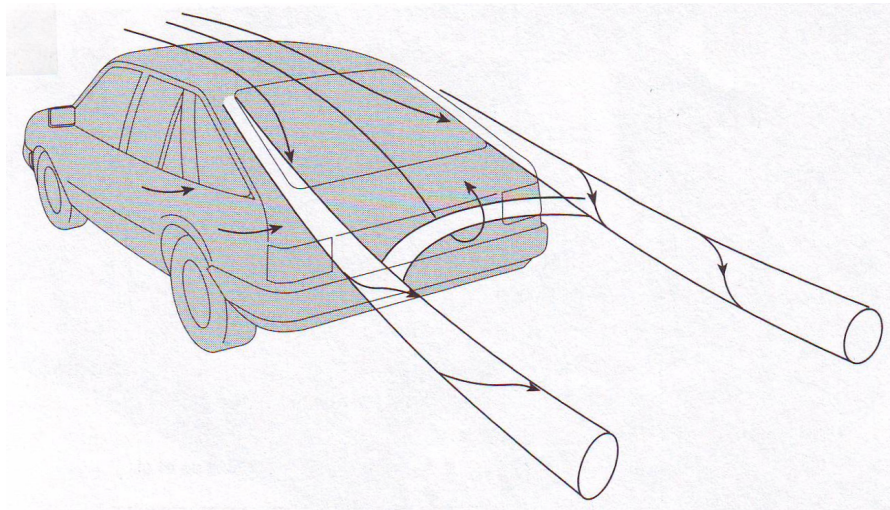


Figure 2.3: Conical vortices are generated at the rear corners creating strong trailing vortices. Figure by Barnard [10].



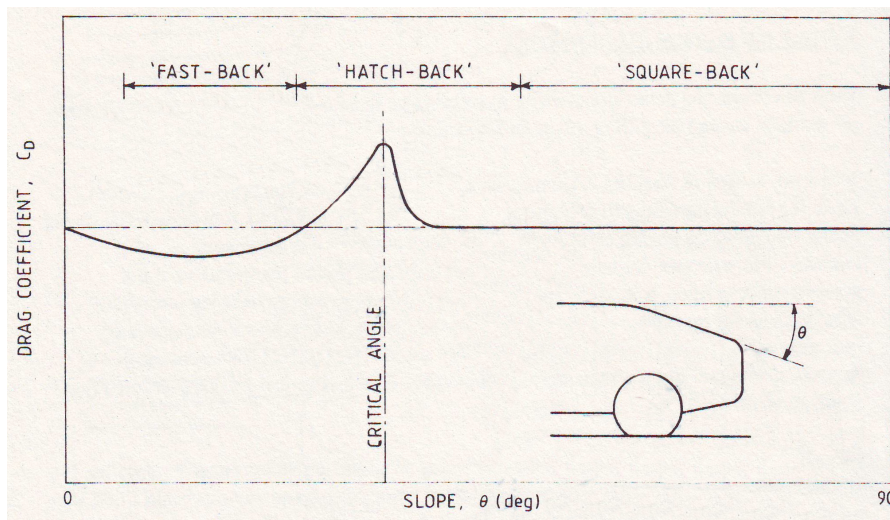


Figure 2.4: Effect of rear body slope on afterbody drag of saloon cars. Figure by Carr [8].

## 2.2 Coefficients of Drag

When designing a normal road-going vehicle, the most important aerodynamic parameter is the drag force [10]. With the substantially lower average speed of a vehicle competing in the Shell Eco-marathon at around 25 km/h, drag is for all intents and purposes the parameter of interest. The drag coefficient can be calculated from equation 2.1.

$$C_d = \frac{F_d}{\frac{1}{2}\rho v^2 A} \quad (2.1)$$

with  $F_d$  being the drag force,  $\rho$  being density of the fluid flowing past the body,  $v$  being the free stream fluid velocity, and  $A$  being the projected cross sectional area of the body.

The  $C_d$  coefficient can be somewhat misleading when comparing vehicles if their projected frontal areas are not the same. A vehicle influenced by a large drag force will show a misleadingly small  $C_d$  when the projected area is also large. For this reason, it is customary to multiply the  $C_d$  with the projected frontal area,  $A$ , to obtain the  $C_d A$  coefficient. In practice this means that if drag force is measured and a coefficient for comparative purposes is desired, the projected frontal area is not of interest, as seen in equation 2.2.

$$C_d A = \frac{F_d}{\frac{1}{2} \rho v^2} \quad (2.2)$$

## 2.3 Vehicles in Cross-winds

During wind tunnel testing, depending on size and technical features of the facilities, the wind is mostly hitting the vehicle head on. This, however, is not necessarily the case in real life, as yawed condition (with yaw angle as defined in figure 2.5) is in fact the prevalent case. A "wind-averaged drag" can be calculated by applying methods of statistical weighting to the yawed case [8]. With low driving speeds, the relative influence of wind velocity on the net airflow direction and speed over the vehicle body is greater than for high speed road travel. For

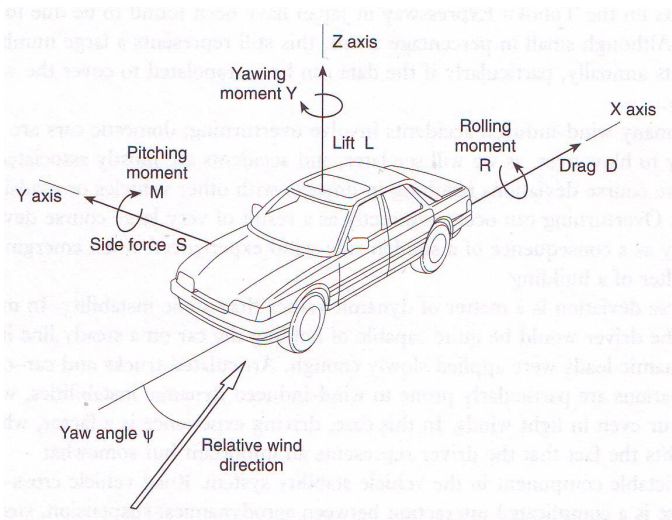


Figure 2.5: Coordinate system.

road safety reasons, good lateral (sideways) stability is important to prevent course deviation [10]. Since correction for yawing forces would be applied by human interaction, it is important that the characteristics of a vehicle in cross-winds are as predictable and stable as possible. For this reason, features such a sharp edge on the D-pillar (see figure 2.1) to provide a consistent line of separation, can be found on vehicles even though they are not necessarily favorable with respect to aerodynamic drag.

A road vehicle exposed to a wind gust acting with centre of pressure at the forward part of the vehicle, will tend to yaw in the direction away from the wind. Since

this would expose a larger area of the vehicle to gusts from that direction, even larger loads can be expected adding to the yawing. As a result, it is desirable to move the centre of pressure aft, which most often will reduce the undesirable tendency of the car to yaw away from the direction of the incoming wind [10]. It should be noted that other characteristics in addition to the aerodynamics of the car, for instance the suspension geometry, play major factors in a road vehicles' response to cross winds. However, this coupling of parameters is beyond the scope of this paper, and only the aerodynamic contribution is therefore mentioned. An extension of the length of the car aft of the rear wheels should move the centre of pressure aft and, based on the reasoning presented above, contribute to making a car less prone to instabilities in severe cross winds. If a comparison of yawing moments on different vehicles is desired, it is important to recognize that it is the moment about the point of neutral response that determines the strength and direction of the yawing response to a side load, not the moment about some arbitrarily chosen axis centre [10]. Even with the same measured aerodynamic yawing moment about an axis system located at the wheelbase centre, two vehicles could have quite different yawing responses if their centre of gravity positions and suspension geometry were different. Reducing lift, or creating down force, as well as having positive pitching moment (nose up, see figure 2.5), are found to improve cross-wind stability [10].

Even though the drag force usually works against the direction of travel (positive drag), situations under which the wind induces a negative drag can in theory occur. When wind angle of attack is yawed due to cross-wind, a component of the lateral force may act in the forward direction along the vehicle axis. If greater than the rearward component of drag due to the forward motion of the vehicle, then the resultant total drag will be negative. This is in theory and not particularly practically relevant. However, a consequence of this is the possibility of higher and lower drag values than that of zero yaw angle at a specific speed.

## 2.4 Diffuser and Ground Clearance

Air will always converge into the gap between car and ground, thus being accelerated lowering static pressure. Up to a certain point, lower ground clearance will in theory increase the acceleration of the air passing through this gap, lowering the static pressure. The distribution of low and high pressures along the underside of a vehicle effects the aerodynamic balance, and might therefore affect the road handling characteristics of the car. Some experiments done on road vehicles of average underbody roughness indicate that with ground clearances of 0,125 – 0,600 times

the wheelbase, a "conventional" car will produce negative lift, or downforce [11]. At ground clearances of less than 0,125 times the wheelbase, the lift becomes positive, which can effect the road holding abilities of the vehicle in an unfavorable manner. This is by no means an absolute solution, but rather an indication that underbody design and roughness along with level of ground clearance are important parameters in creating the amount of lift generated by a road vehicle. Race cars will often have very low ground clearance along with high values of negative lift, proving the point that the two are not mutually exclusive. If calculations and simulations of underbody downforce effects are desired, it is important to appreciate that viscous effects may play a dominant role in the nature of underbody airflow [11].

If the underbody geometry creates a low pressure region under the vehicle, then higher pressure air from the surroundings will migrate to this region from the sides. In such a situation it is favorable to have sharp joins from the bottom of the tunnel wall to the outer portion of the floor, since this has the effect of creating a vortex within the underbody which lowers the static pressure, assisting with maintaining attached flow [11].

## 2.5 Implications of Theory

Due to the monocoque design, i.e. the chassis is integral with the body, of the existing vehicle, bodywork removal was not possible. For this reason the maximum rake angle (as discussed in section 2.1) was given. Altering lines of separation by changing edges and contours would be possible by adding to the bodywork. Surface roughness of the existing body could quite extensively be altered without compromising structural integrity, with weight as the main limiting factor.

The minimum ground clearance and low average speed, 10 cm and 25 km/h respectively, imposed by regulations as introduced in section 1.4, influenced the extent to which a diffuser and ground clearance could affect the aerodynamic performance of the vehicle. However, the underbody design was found to have a potential for improvement, as discussed in sections 4.5 and 4.10.

# Chapter 3

## Test Methods

The ideal method of testing and exploring car aerodynamics would be road testing in natural conditions. Only then can all factors affecting the aerodynamics, such as rotating wheels, natural atmospheric wind conditions and underbody flow conditions, be completely accounted for. However, road testing has several challenges to surmount, especially regarding problems with separating drag measurements from rolling resistance, frictional and mechanical losses. Also, the equipment has to be carried with the car, which causes practical problems. Road testing was found impractical for the purposes of this project, and will not be further discussed. The two main alternative test methods, which are the most commonly used in aerodynamic development and testing of cars, are Computational Fluid Dynamics (CFD) and wind tunnel testing. These methods will be elaborated in this chapter, and also a discussion of application in this project will be given.

### 3.1 CFD

The use of CFD in car aerodynamics has increased rapidly the recent years as computers have become more powerful. One of the great benefits by using CFD is that you can easily visualize and analyze pressure and velocity fields, which makes it ideal in the early design process where different shapes are considered. CFD can give a good indication of where separation and vortex generation are likely to occur on a vehicle [10]. It is also widely used to study internal airflows in vehicles, which can be difficult to calculate and simulate in other ways. Unfortunately, there are also downsides in using CFD. Since the aerodynamic drag is very dependent on where the flow separation takes place, it demands high accuracy in the calculations to get good, reliable results. To achieve this, a very fine and precise grid

must be generated, which can take a skilled user a considerable amount of time. Then, costly processor time is needed to solve the problem numerically. This can take several days or even weeks if a highly accurate solution is demanded [10]. However, the disadvantages mentioned are basically only limited by the computer capacity, which is still rapidly increasing. The most processor-demanding CFD process is termed Direct Numerical Simulation (DNS), where an extremely fine grid is used such that Navier-Stokes equations can be solved for even the smallest turbulent eddies [12]. Currently, DNS can not be applied to industrial problems, only for conceptual studies of turbulence. Therefore it is more common to use turbulence models to solve the Reynolds-averaged Navier-Stokes (RANS) equations, which gives time-average solutions that are accurate enough in most industrial applications.

## 3.2 Wind Tunnel Testing

Wind tunnel testing has the big advantage that once the vehicle model is produced and rigged in the wind tunnel test section, it can quickly provide highly accurate data. Data for different boundary conditions, such as different wind speeds and yaw angles, can be acquired quickly. If similar changes in conditions are done on a computer model, the whole simulation has to be run over again for each case. On the other hand, wind tunnel testing can be both highly costly and time consuming. The wind tunnel itself is a huge investment, and the production of prototypes can be very expensive. Small changes in design will take much more time to implement on a physical prototype than on a computer model. The accuracy of the wind tunnel measurements is affected by several factors, including blockage, scaling effects and the moving road problem, and the reliability and the validity of the data need to be evaluated in each case. Some of the major error sources will be discussed in the following.

### 3.2.1 Blockage

Blockage is one of the main error sources in wind tunnel testing. For a closed-section tunnel like the one at NTNU, the car will block a certain part of the test section area and make the flow area smaller. We can easily see through mass conservation,  $\rho AV = \text{constant}$ , that the flow will be accelerated around the car. Hence, the drag will be overestimated, and the error will rapidly increase with the blockage ratio, as shown in figure 3.1. A drag coefficient formula corrected for solid blockage can be developed using equation of continuity [10]:

$$V(\text{true}) \times (S - A) = V(\text{indicated}) \times S \quad (3.1)$$

where  $V(\text{true})$  is the actual speed around the model,  $V(\text{indicated})$  is the speed of the undisturbed flow upstream of the car,  $S$  is the test section area, and  $A$  is the projected frontal area of the car.  $\rho$  is assumed constant and eliminated. By solving the equation for  $V(\text{true})$  and inserting it into the drag coefficient, we obtain

$$C_D = C_D(\text{indicated})((S - A)/S)^2 \quad (3.2)$$

However, this formula does neither take into account blockage effects due to wake displacement nor the fact that the corrected drag coefficient is calculated using the *maximum* cross-sectional area. In 1986, E. Mercker [13] developed a more advanced correction expression based on H. Glauert's [14] and E. Maskell's [15] work which included blockage effects due to flow separation. Mercker's formula can be expressed as

$$C_D = C_D(\text{indicated})(1 - A/S)^{1,288} \quad (3.3)$$

The constant 1,288 was determined empirically by testing of a standardized MIRA car model in three differently sized test sections at DNW (German-Dutch Wind Tunnels). The correction expression was tested in yaw angles up to 30° with satisfying results.

Even though correction methods have improved, different methods still give different results. It is therefore advised to keep the blockage ratio as small as possible [16]. The maximum recommended blockage ratio varies in literature between 5 % and 10 % [9] [10]. The blockage ratio and the implications of it in this project will be thoroughly discussed in section 4.7.1.

### 3.2.2 Small Scale Testing and Reynolds Effects

The use of scale models in wind tunnel testing in the design process of cars can be both cost and time saving, but it needs to be done properly. The main restricting parameter is the Reynolds number  $Re$ , which should be equal for the model and the full-scale car, i.e.

$$Re = \left( \frac{\rho V l}{\mu} \right)_{\text{model}} = \left( \frac{\rho V l}{\mu} \right)_{\text{full-scale}}, \quad (3.4)$$

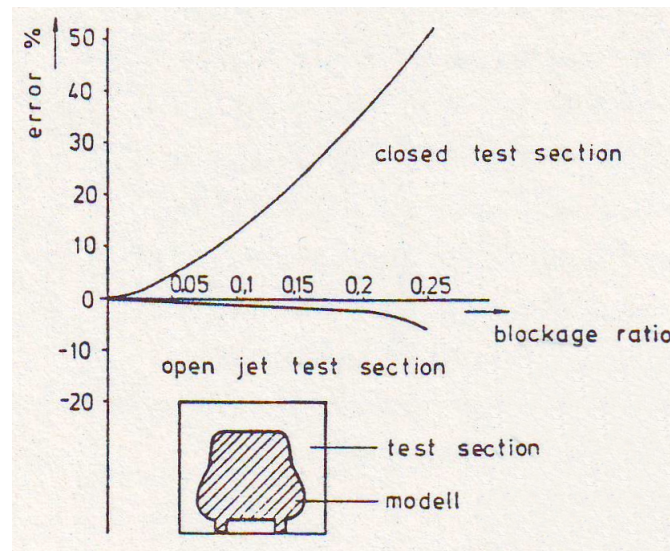


Figure 3.1: The error due to blockage increases rapidly with the blockage ratio. Figure: C. Kramer [16], based on work by W. Wuest [17].

where  $\rho$  is the air density,  $V$  is the free stream velocity,  $l$  is the characteristic length, in literature commonly based on either the length or the width of the car, and  $\mu$  is the dynamic viscosity.

If the two models were put in a flow with the same properties, the skin-friction drag would be lower on the model than on the full-scale car [10]. The reason for this can be explained by looking on a flat plate in two different sizes. The transition from laminar to turbulent boundary layer will occur at the same absolute distance from the leading edge in both cases, but a greater percentage share of the large plate will be covered by turbulent boundary layer. As mentioned earlier in section 2.1, and illustrated in figure 2.2, the skin-friction coefficient is higher for the turbulent boundary layer than for a laminar one, and hence the large plate will experience higher friction drag per unit length than the shorter one.

The main problem with small-scale testing is to produce high enough wind speed to achieve the same Reynolds number as for a full-scale car. If both are tested in equal air conditions, one can for instance see that for testing of a 1/5 scale model, the wind speed has to be five times the full-scale test speed. In order to simulate a normal passenger car at e.g. 120 km/h, the wind tunnel speed has to be 600 km/h when testing the scale model, which is far more than normal automotive wind tunnels can achieve. Different techniques, such as pressurizing the wind tunnel to increase the density or altering the viscosity by cryogenic cooling [10], are possible but very expensive. The best way to avoid the problem is to have a



large wind tunnel large enough for full-scale testing, and most of the major car manufacturers are in possession of one or have access to one. When a scale model is used and the full-scale Reynolds number is not achievable, the wind tunnel is usually run at maximum speed to get as close as possible [9]. If the flow stays attached at the lower Reynolds number, then it will stay attached in the full-scale vehicle's Reynolds number as well. That is due to the nature of boundary layers: A turbulent boundary layer will have much higher momentum transfer than laminar flow, and can withstand higher adverse pressure gradients than a laminar boundary layer. Hence, a turbulent flow can either avoid separation completely, reattach separated flow or move the separation point on the vehicle's rear part aft. The point of flow separation is very sensitive to the Reynolds number in a certain range, often between  $Re = 10^5$  to  $10^6$ , which also is a typical range for automobiles [9]. Therefore, if the flow separates in case of the low Reynolds number, the drag can be drastically lower in case of a larger Reynolds number if the increase leads to reattachments and a narrower wake due to longer attached flow. A design developed from a scale model can then be far from optimized in terms of drag reduction.

A 1:4 scale model was made of clay, scanned and converted into a CAD-model by the PureChoice-team in 2008, as a basis for further optimization of the design. The clay model was considered used this year to examine new end extensions before creating a full-scale prototype. However, due to the above mentioned effects and the fact that a full-scale was available, it was considered as inappropriate use of time.

### 3.2.3 The Moving Road Problem

Another error source in wind tunnel testing of cars is the fact that the test section floor is standing still, such that the air has a relative motion to it. In real life, under calm conditions, the air is standing still relative to the road. A boundary layer will be developed along the floor in the test section and partly enclose the model, which will lead to different flow conditions than on a road. There are mainly three methods used to correct for this; ground board, moving belt and the suction method. The easiest and cheapest method is the use of ground board, where the car simply is lifted out of the boundary layer. This can give satisfactory results in testing of passenger cars, but is generally not considered good enough for race car testing. A typical moving belt setup can be seen in figure 3.2. It is a popular method within the race car industry, but also Volvo has invested in a moving belt wind tunnel to optimize testing of their passenger cars [18]. However, there are some problems to overcome, including supporting the car without interfering

the flow and various mechanical challenges with the belt [10]. A simpler and less expensive method is to apply suction under the car to reduce the boundary layer, which is a quite popular approach in many wind tunnels [9]. The wind tunnel at NTNU has neither moving belt installed, nor a device for applying suction. Hence, a ground board was the only available method in the experiments.

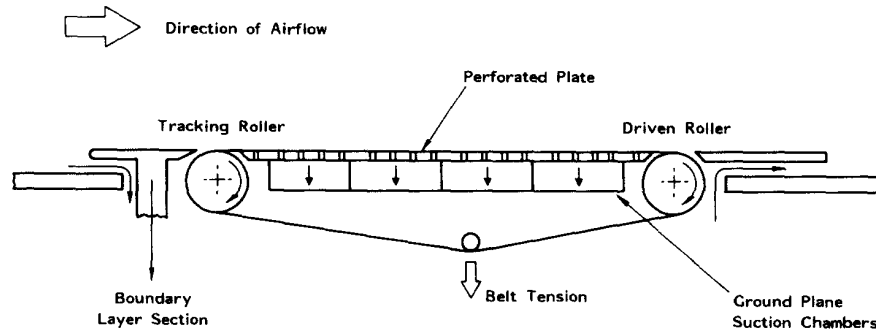


Figure 3.2: A moving belt is used to avoid errors due to the boundary layer that is developed in the test section. Figure by K. Burgin [19].

### 3.2.4 Visualization

A very popular method to visualize the flow around the vehicle is to attach small wool tufts on the car's surfaces, which was done in this project and can be seen in figure 4.7. In the case of attached flow the wool tufts will stick to the surface in the flow direction, while turbulent spots and vortices will be revealed by flailing tufts. Another method is the use of smoke, even though it can be hard to get useful results out of it, especially by only looking at the smoke passing the car. However, separation can be revealed by leading the probe into the wake behind a possible point of separation. If separation occurs, the smoke will tend to be drawn forward against the free stream flow direction due to the reversed flow direction, as illustrated in figure 3.3. Smoke was used a couple of times during the wind tunnel sessions, but mostly as show-off for media.

## 3.3 CFD and Wind Tunnel Testing in This Project

For several reasons, the prioritization in this project was to only use wind tunnel testing. First of all, as mentioned earlier, it can take an experienced CFD-code user weeks to generate a proper numerical mesh and run the simulations. Taken

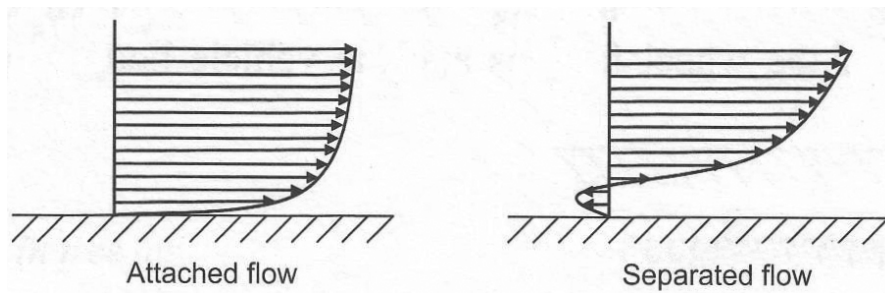


Figure 3.3: Attached versus separated flow. Figure by J.J. Santin et al. [6].

into account the limited time schedule from startup in January to the Shell Eco-marathon competition May 5th, a CFD study would have been wrong prioritizing. Secondly, the car was already produced and only smaller optimizations of the current design was possible. Since drag is very dependent on flow separation, and even small changes in design can severely change the points of flow separation on the car, a very good CFD model had to be developed to get anything valuable out of the simulations. Finally, full scale testing of the car was possible in the large wind tunnel at the Aerodynamic Lab at NTNU, and despite blockage effects and other error sources, the testing could provide very useful data. The case would have been different if the car was to be designed from scratch. In that case, use of both wind tunnel and CFD would have been a very good combination, a commonly used work flow in the car industry [9] [10]. The team behind the current world record holding car in the Shell Eco-marathon Prototype class, PAC-car II, used CFD extensively in the car design process, and used wind tunnel for validation and testing purposes [6].

# Chapter 4

## Presentation of Work

### 4.1 Areas of Improvement

#### 4.1.1 Surface Friction

From the combination of the theory of decreasing coefficient of friction as flow speed increases (see section 2.1) and the low required speeds of the Shell Eco-marathon, the surface was identified as an area of interest. From the point of view of airflow over the surface of the car, the carbon fiber finish was quite rough. During the two preceding years of participation the car has been covered in a thin plastic film, primarily for esthetic reasons. This solution was considered not to be optimal for reducing friction. It does not provide a particularly smooth surface, as well as being difficult to apply perfectly on the curved shape of the car. A completely different aspect of finding a solution to the problem of surface finish was the desire to have the team graphic profile on the car. This had not previously been done, and would by all accounts be very difficult to accomplish with a surface treatment in the form of the thin plastic film. Some sort of paint was an obvious alternative. However, it would not necessarily result in a smooth finish even though it most likely would be a flexible solution to the graphical profile. After some research it was decided to hand a sample piece of carbon fiber to a local paint shop by the name of Falkenberg Bil. The result was found to provide a highly satisfactory finish. With a process of grounding the surface, dusting it down until parts of the carbon fiber were almost in the open, and lastly spray painting, the unevenness of the carbon fiber body was all but completely gone. By using a professional paint shop, the result with respect to both aerodynamics and esthetics was considered satisfactory.

### 4.1.2 Protuberance Drag

Being unable to change the shape of the car turned out not to be a significant problem for any work intended to improve aerodynamic performance. By using wool tufts on the surface of the car when conducting wind tunnel tests, especially at the rear most part, it was established that the flow was indeed attached for flow speeds of up to 35 km/h. This was the case both with the end extension of 2009 mounted and without. Since the flow followed the top curvature of the end extension nicely, it was decided relatively early on that using the same top design would be rational with the time constraints in mind. However, the 2009 solution of sealing the underbody tunnel increased the frontal projected area. Continuing the existing underbody tunnel into an end extension with upper surface similar to the 2009 end extension could prove to be a better solution.

As discussed in section 2.1, open wheel wells create drag that can be reduced simply by covering them. The rear wheels of the car have been covered since 2008, but the front wheels have not. Since the front wheels necessarily need to be able to protrude outside the body of the car, a wheel cover would have to allow for this movement. Due to the members in charge of the mechanics experiencing difficulties with the door, the front wheel cover was restricted in the aft direction by the door. The following spatial restrictions existed:

- Forward restriction by the front of the car
- Rear restriction at the door

It is desirable to have the covers as narrow as possible, so that they create as small a contribution as possible to the projected area of the car. They should also curve gently so as to maintain attached flow. With the restrictions at hand, there was little room for variations in shape and design. 3D drawings of the end result is shown in figure 4.1.

It should be noted that the maximum deflection of the front wheels on this vehicle was only about 9 cm protuberance outside the vehicle body, allowing for quite narrow covers. Even though the 3D models were finished and prepared for milling, these wheel covers were prioritized away and never built. This was due to high demand on the milling machine, manpower needed for production of remaining vital components, and that without the large wind tunnel there was no way of determining if the covers would be favorable.

Even though the extent to which front wheel covers would impact the aerodynamics with respect to drag forces is not known, it is assumed that they would prove beneficiary, especially in yawed condition. This is based on the fact that the more



Figure 4.1: 3D model of front wheel covers.

yawed the wind direction is onto the car body, the less the covers will add to the effective projected area of the car, and would rather represent a better rounded surface. It is important to emphasize that these are mere speculations and a definitive answer can not be obtained based on the work conducted for this report.

As mentioned earlier, rear wheel covers were used by both the 2008 and 2009 teams (seen in figure 1.2). However, due to a problem with the wheel suspension, the rear wheel containing the electrical motor unintentionally protruded the vehicle body. This was discovered as late as after arrival in Germany, and effectively prevented the use of the rear wheel covers.

### 4.1.3 Driver Ventilation

The PureChoice team of 2008 originally had no ventilation system for the driver of the car which led to problems with heat and dew inside the car during races. A quick solution performed on site in France was to drill three holes in the windscreen and three holes in the side window. This did have some effect, but since it was not considered a satisfactory solution, it was recommended that the 2009 team thoroughly look into the issue. In spring of 2009 an Experts in Team group created the report *Eco-marathon Driver Performance* [20], in which Knut Omdal Tveito used Computational Fluid Dynamics to analyze ventilation of the driver cabin. Mass flow of air required to handle the heat generated by a human in the car in sunny weather was estimated along with design suggestions for a system of ventilation. Tveito concludes the report by suggesting a submerged NACA inlet below the wind screen and a reversed NACA duct on the roof as outlet. Estimated

flow rate increase was 58,5 times with similar level of drag compared to that of the provisional holes of the 2008 team. There certainly was a desire to solve the heat problem on this years car. With the promising results of Tveito's report, which are the only thorough work of its kind on the car, it was considered the best option. However, as Tveito notes in the conclusion of the report, wind tunnel tests should be conducted of the design to verify the results. In order to perform verification tests of the design with a satisfactory level of precision, extensive modifications to the monocoque would be involved when building the inlet and outlet into the car body. Problems would arise if the tests turned out to show a larger increase in drag than what could be considered acceptable for a feature that does not improve performance for the purposes of the competition. Time constraints meant that if the results did reveal too large negative effects, time would be highly scarce for setting the car back into its original state. Actual construction of the system, as well as the computer modeling of it, would rest on the shoulders of the authors of this paper, none of whom had any experience with this kind of work. Especially learning computer-aided design (CAD) was expected to take a substantial amount of time, and with the necessity for a new end extension established early on in the project, focus and attention was placed on getting that product out in real life. Since the experience in the above mentioned fields gained while working towards a new end extension would be directly transferable to a possible ventilation system, the decision whether or not to implement it was delayed until a better perspective on time was available. A ventilation system, based on the work of Knut Omdal Tveito or otherwise, was eventually rejected due to lack of time.

#### 4.1.4 Fuel Cell Ventilation

In the hydrogen fuel cell stack air is both the oxidant in the chemical reaction as well as the medium for cooling. Hence, the required amount of air will vary with electrical load and stack temperature. Working out and specifying the airflow requirements was the responsibility of group member Lorenz Baur in collaboration with group member Torstein Skarsgard. However, since this necessarily means some sort of inlet and outlet arrangement, an impact on the flow around the vehicle could result, changing its aerodynamic performance. For this reason some investigative work was done.

To drive the air through the system, a pressure drop is needed. Hence, the intake should be placed at a location where the air's energy is high so that it can be converted to high static pressure [11], such as at the front of the car. This would imply some sort of ducted arrangement for transporting the air aft to the the fuel cell stack. Possible positions considered for an outlet were in the wheel wells, in the

roof or at the rear. A rear end solution was quickly rejected due to the complicated nature of the vehicle body resulting when the end extension was subsequently to be mounted. In addition to the body design, the intention was for the vehicle to be able to be displayed without the end extension all together, requiring a detachable solution complicating an outlet. Roof mounted outlet was rejected based on the uncertainty concerning how it would effect the flow over the roof and if it could induce premature separation. A wheel well based solution would certainly not disturb any neatly attached flow field, and is considered a good alternative placement for outlets [10]. The final solution was placing both the intake and outlet in the wheel wells. This means that the air will not, due to placement in practically equal pressure regions, naturally flow through the system, producing the need for an artificially driven airflow. This was accomplished by mounting a radial fan on the stack attached to tubing from and to the wheel wells as seen in figure 4.2.

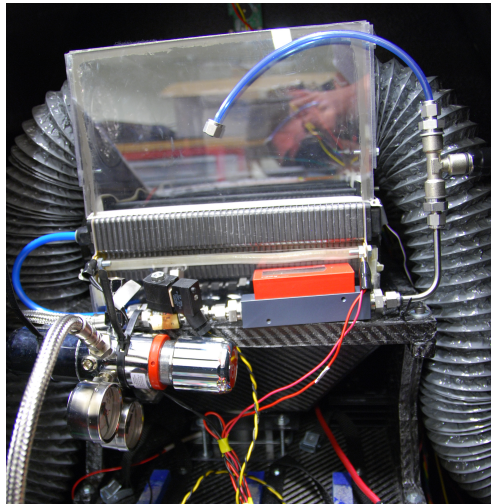


Figure 4.2: Fuel cell with ventilation tubes in gray.

## 4.2 Experimental Setup

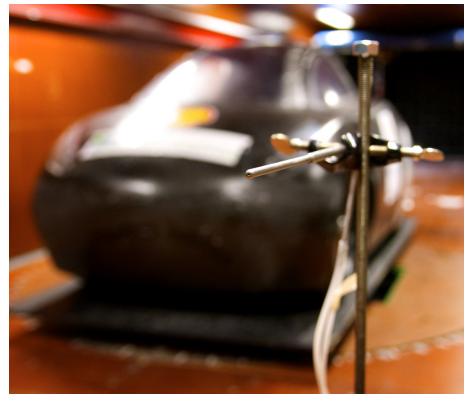
The experiments were conducted in the large wind tunnel at Norwegian University of Science and Technology. Inside the tunnel, a plate large enough to hold the car was mounted on top of a metal rig attached to a scale as shown in figure 4.3 and described in section 4.3.3. Holding the car in place was two pieces of wood placed behind the rear wheels, along with two placed in front of the front wheels. Even



though the scale could be rotated, the length of the car compared to the width of the tunnel effectively constrained the maximum possible yawed inflow angle to just above  $15^\circ$ . Flow speed measurements were conducted using a single pitot static tube located upstream of the car as shown in figure 4.3(b). The pitot tube was connected to the same computer as the scale via a pressure transducer.



(a) Vehicle in wind tunnel, 01.02.2010.



(b) Vehicle and pitot static tube 16.02.2010.

Figure 4.3: Wind tunnel test setup.

## 4.3 Experimental Equipment

### 4.3.1 Wind Tunnel

The large wind tunnel at NTNU has a test section with dimensions 2.7 m x 1.8 m x 11 m, and is powered by a 220 kW centrifugal fan, capable of achieving wind speeds up to 30 m/s. The test section has a six-component balance, described in Section 4.3.3, that can be rotated a whole  $360^\circ$  to simulate the effect of wind approaching at an angle.

### 4.3.2 Pitot

The pitot tube used is an ordinary pitot static tube, the specifics around which can be found in reference [21]. It is connected to an electronic pressure transducer that produces an output voltage which is recorded by a computer. This voltage is a representation of the actual difference in air pressure between the two pressure

points. The purpose of calibrating the pressure transducer is to determine the relationship between  $V$  outputted by the transducer and the pressure difference in Pa. In other words; the result of this calibration is a constant with units Pa/V.

The procedure of calibration conducted is as follows. Each of the two tubes from the pitot need to be connected to the electronic transducer and a manometer at the same time by splitting them (as illustrated by figure 4.4). This allows the pressure difference between  $P_{stagnation}$  and  $P_{static}$  to be captured by both the manometer and the the electronic pressure transducer. The next step is to make sure the manometer is placed completely horizontally and adjust it such that it reads zero mm when the wind tunnel is off and the wind speed is zero. By taking readings of voltage from the transducer, and readings of mm fluid displacement from the manometer at different wind speeds, the relationship calibration constant may be obtained. Actual pressure difference in Pa is calculated from equation 4.1. The wind speeds during calibration are chosen so that they cover the range of speeds used in the actual experiment. Due to the phenomena of hysteresis [21], measurements are taken with wind speeds increasing as well as decreasing. For each wind speed, the actual pressure difference (determined from the manometer) is plotted against the corresponding voltage from the pressure transducer, as shown in figure 4.3.2. The desired relationship is determined by linear regression.

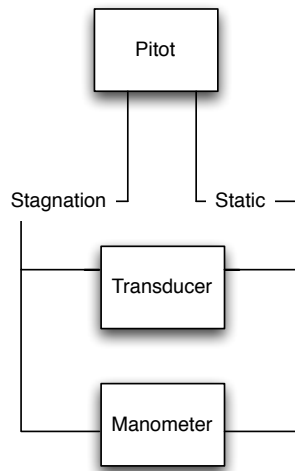


Figure 4.4: Pitot calibration setup schematic.

$$\Delta p = \frac{\rho g h}{5} 10^{-3} \quad (4.1)$$

where  $\rho = 800 \text{ kg/m}^3$  is the density of the fluid in the manometer,  $g = 9,81 \text{ m/s}^2$ .

The factor  $\frac{1}{5}$  is due to the inclination of the manometer.

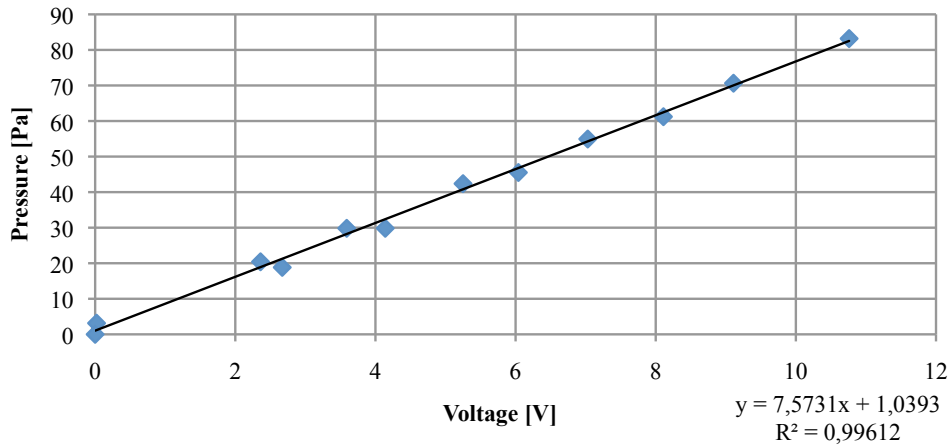


Figure 4.5: Pitot calibration constant.

This constant (7,57 in the case of figure 4.3.2) is given as an input to the logging software which uses it to convert voltage into pressure, and then calculate the velocity from equation 4.2 which is presented as the output to the user.

$$U = \sqrt{\frac{2(p_{\text{stagnation}} - p_{\text{static}})}{\rho_{\text{air}}}} \quad (4.2)$$

To check that the speed value given by the logging software is correct, a reading at some wind speed can be taken from the the manometer, and the wind speed is calculated manually using equation 4.2.

One important note is the use of amplifiers. If amplifiers are used, the raw voltage due to a change in pressure can be obtained from equation 4.3.

$$V_{\text{raw}} = \frac{V_{\text{measured}} - V_{\text{offset}}}{\text{amplification}} \quad (4.3)$$

In equation 4.3,  $V_{\text{offset}}$  is the voltage output from the transducer at zero actual wind speed, and amplification is the value chosen at the amplifier. Since the input to the computer logging software was the amplified values, the calibration constant used was also determined from equally amplified values.

### 4.3.3 Scale

The scale has six electronic load cells, three for measuring vertical loads and three for measuring horizontal loads. Calibration of the scale is essentially the same process as for the pressure transducer. During calibration the entire setup, including vehicle and rig, was in place on the scale. External loads of 1 kg, 2 kg and 4 kg were applied to each of the six load cells individually. For the first test of 01.02.2010 the range of weights was roughly based on figure 4.6 [10]. This was later based on the obtained drag results from previous tests. The values in kilograms are multiplied with the gravitational acceleration and, as was explained in section 4.3.2 for the pressure transducer, points from the weights in Newton and their corresponding values in V from the load cells give the data from which the constant in units  $N/V$  is determined. Drag, lift, side, yaw, pitch and roll may then be calculated correctly based on the voltage from each of the cells when loaded. Verification of the scale calibration can be performed by pulling the vehicle with a known load.

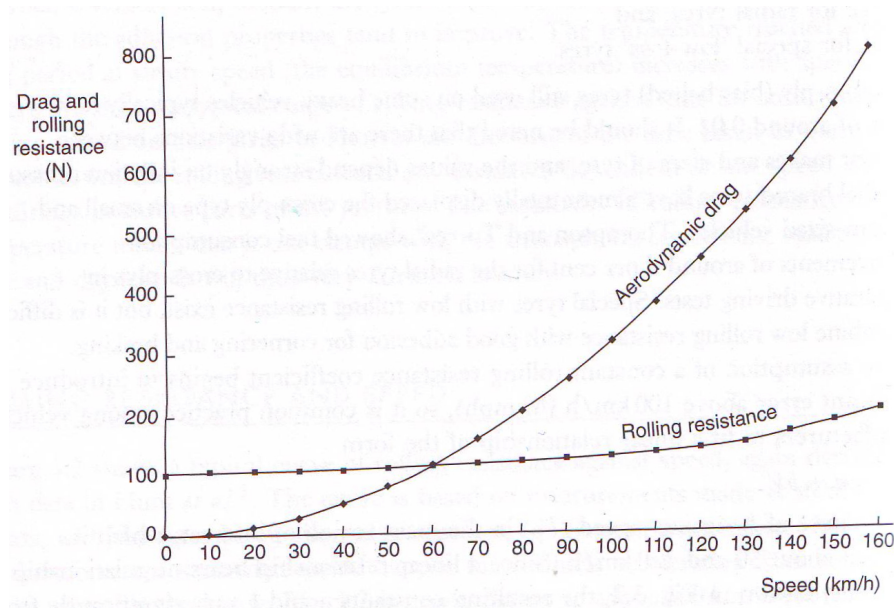


Figure 4.6: The variation of rolling resistance and aerodynamic drag with speed for a typical medium-sized European car. Figure by Barnard [10].

### 4.3.4 Labview - Forcelog

Forcelog, a Labview program, calculates all forces and moments along with wind speed based on the voltage from each cell, the pitot and the corresponding calibration constants. This was the main application for recording results during experiments. In addition to Forcelog the Labview application Genlog was used, primarily for calibration and validation purposes, as it merely displays the voltage outputs. Both Genlog and Forcelog required the voltage input to lie between  $\pm 10$  V which restricted the extent to which the signals could be amplified, as discussed in section 4.3.5.

### 4.3.5 Amplifiers

Each voltage output from the load cells were connected to an amplifier. The amplifiers were used to tune the output signal in such a way that they would lie between the  $\pm 10$  V limit, as mentioned in section 4.3.4, during the duration of the experiment. This was done by adjusting the output signal from each load cell such that they would lie in the lower part of the range when no additional load than the weight of the car was applied, and in the upper part of the range when an additional 4 kg (plus weight of the basket) was applied to the cell. Adjusting amplification on each output signal will necessarily affect the value of the calibration constant. As such, once the calibration constant is obtained, the amplification cannot be adjusted without performing a new calibration of the corresponding signal.

## 4.4 Test Procedure

The wind tunnel tests were performed at three different wind speeds, namely 25 km/h, 30 km/h and 35 km/h, or equivalently 6,9 m/s, 8,3 m/s and 9,7 m/s. The wind speeds were chosen based on the average speed during the race, that would be between 25 km/h and 30 km/h. The reason why three different wind speeds were chosen was to ensure that there was no sudden changes in drag coefficient around the operational vehicle speed due to e.g. separation. In addition, the car was tested at yaw angles  $0^\circ$ ,  $8^\circ$  and  $15^\circ$  (yaw angle as defined in figure 2.5), which is a typical range for automotive testing [22]. The unstable wind conditions at Eurospeedway, Lausitz [23] and the low speeds the car operates in makes it extra important to ensure nothing severe will be changed in yawed conditions. The relative wind speed angle will be more vulnerable to side wind at such low cruise speeds, as discussed in section 2.3.

In the first test, the forces were measured and averaged over a period of 10 s with sampling frequency 30 Hz, giving a total of 300 samples. However, this turned out to give unsatisfying consistency in the logged results. A good consistency was obtained by doubling the number of samples to 600, still at 30 Hz, which then was used in the following two tests.

The car was tested in three different configurations, which in the following text will be referred to as "PureChoice", "Fuel Fighter 2009" and "Closed tunnel". The PureChoice-configuration is the car in its original shape from 2008, cf. figure 1.2(a), while last year's car will be referred to as the Fuel Fighter 2009-configuration. A picture of the latter can be seen in figure 1.2(b), where one can notice that the tunnel underneath is closed and that an extension is mounted on the rear part of the car. The mirrors are mounted inside the driver's compartment in all three configurations despite the external mounting in 2008, because it was considered more interesting to only look at the effects of the extension and the closed tunnel. The closed tunnel-configuration is the same as the Fuel Fighter 2009-configuration, but without the end extension.

## 4.5 Wind Tunnel Testing

A total of three sessions of wind tunnel testing were performed. The initial test was done to get a brief idea of the difference between the previous car configurations, to map potential error sources, and to get an understanding of how calibration, setup and adjustments of the equipment worked. The results of the test will be discussed later, but it was decided not to use them in the drag calculations due to too many possible sources of errors. One of them being the placement as shown in figure 4.7, which was due to other ongoing wind tunnel experiments. However, in spite of the error sources, a good qualitative understanding of the difference between the two last years' configurations was obtained, as well as practical experience in wind tunnel testing. Wool tufts and smoke was used to examine flow separation.

The purpose of the second wind tunnel test was the same as the first one; to map the existing aerodynamic properties of the car in different configurations, but with improved setup. This would also make the background for the prototype production. Based on literature study, a hypothesis was set up in advance of the first wind tunnel test regarding the expected effects of the changes made in 2009. The extension was expected to give a positive contribution to drag reduction because of delayed flow separation and hence a smaller wake, provided that the flow stayed attached until the end of the car. The closed tunnel was on the other hand expected to give an increase in drag due to larger frontal area and



Figure 4.7: The rig was positioned at the rear most position in the wind tunnel, which could affect the wake and hence the drag measurements of the car.

larger wake area behind the car. The hypothesis was confirmed by the results of the second wind tunnel test, given in figure 4.8. The positive effect of the extension was approximately cancelled by the negative effect of closing the tunnel, and the measured drag on the 2008 and the 2009 car was very close in magnitude. Notice though, that the drag must have been slightly higher than measured on the PureChoice car due to the external mirrors which now were removed. The  $C_d$ -values in figure 4.8 are higher than expected, but are not corrected for blockage. This will be described later.

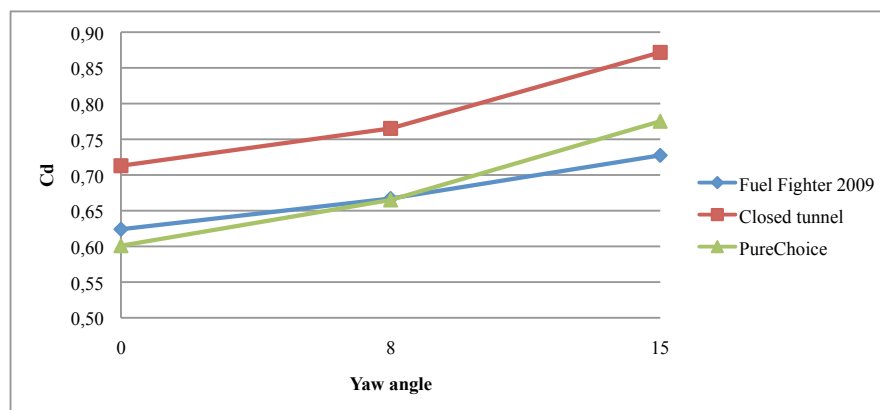


Figure 4.8: The second wind tunnel test (16.02.2010) proved that the car extension gave a positive effect in terms of drag reduction, while closing the tunnel led to increased drag.

### 4.5.1 Extension Prototype

Flow visualization by wool tufts showed no sign of separation on the upper side of the car or the 2009 extension. Therefore, it was decided to keep the shape of the upper part from last year. The tunnel underneath the car was determined to be extended through the extension with the same angle as the tunnel angle at the end of the car. The sides of the extension and the angle of the tunnel side walls were supposed to be quite rounded and curved, but was for practical reasons cut almost with no curvature on the prototype. Styrofoam was chosen as prototype material because of its favorable processing properties. It is also a light material, which made the prototype easier to handle and mount on the car.



Figure 4.9: The finished extension prototype.

## 4.6 Calculation Inputs

The drag of the plate was subtracted in all calculations. The car was placed on the test section floor just clear of the plate to get approximately the same blockage and flow conditions when measuring the drag, which is a method used i.a. in an equivalent wind tunnel at Cranfield Institute of Technology, England [22].



Input Data	Closed Tunnel	Open Tunnel
Density	1,23 kg/m <sup>3</sup>	1,23 kg/m <sup>3</sup>
Projected frontal area	0,94 m <sup>2</sup>	0,90 m <sup>2</sup>
Test Section Area	4,86 m <sup>2</sup>	4,86 m <sup>2</sup>
Continuity correction	0,651	0,664
Mercker correction	0,758	0,768

Table 4.1: Input data used in the  $C_d$ -calculations.

### 4.6.1 Projected Frontal Area

The projected frontal area of the car was calculated in two different ways, both by using the existing CAD model. The PureChoice team was concerned that the real car was a bit smaller than the CAD model due to milling problems. Therefore, last year's team performed a 3D-scan of the model to verify this [24]. However, it turned out that the error was negligible such that the CAD model could be used in further work. The first method to calculate the projected area was by exploiting the wall between the driver compartment and the fuel cell compartment. The wall was somewhat enlarged to fit the projected area of the car, and the area of this was calculated using the CAD-software Inventor. The area of the wheels was added. The result of this calculation was 0,89 m<sup>2</sup> for the PureChoice-configuration, and 0,94 m<sup>2</sup> for the Fuel Fighter 2009-configuration. This was somewhat higher than calculations done by the 2009-team, which estimated the projected frontal area to be 0,74 m<sup>2</sup>. Therefore, another calculation was done to decide which estimate to use. A picture was exported to Adobe Photoshop where a black and white picture with the exact same width and height as the car was created (figure 4.10). A MATLAB-script was created which counted the number of black pixels and calculated the projected area using the following:

$$A = \frac{n_{\text{black pixels}}}{n_{\text{total pixels}}} W_{\text{real}} H_{\text{real}}, \quad (4.4)$$

where  $A$  is the projected frontal area,  $W_{\text{real}}$  and  $H_{\text{real}}$  are the width and the height of the car, respectively. The results confirmed what found using the first method, and the frontal projected area was decided to be 0,90 m<sup>2</sup> for the PureChoice-configuration and 0,94 m<sup>2</sup> for Fuel Fighter 2009-configuration. The latter is also used as projected area in experiments done with new rear extensions, since the frontal area is unaffected by the modifications.

In literature, differently defined projected areas for yawed angles are used. However, most commonly used is the projected frontal area at 0° yaw angle for all yaw

angles [10]. This is also in accordance with what stated by SAE [25], where the x-axis is fixed to the car and the frontal area is the vehicle area projection in the x-direction.

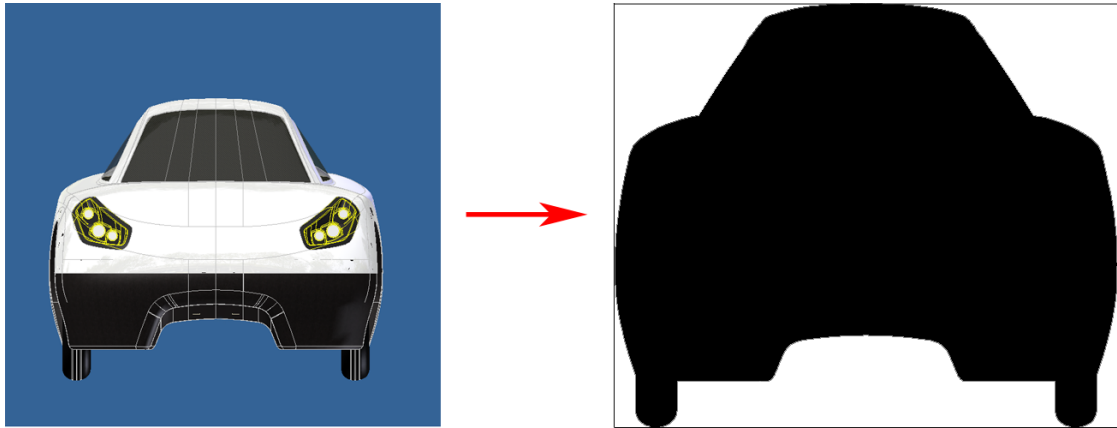


Figure 4.10: The projected area was calculated using a Matlab-script based on a black and white image of the car.

## 4.7 Results

Figure 4.11 shows the results obtained for the PureChoice-configuration in the three different wind tunnel tests. The figure confirms what discussed in section 4.5, that there were too many error sources and too high inconsistency in the measurements to use them in further drag calculations. The difference was more than 50% at the largest yaw angle. It was also observed an undesirable difference of approximately 5% between the two last tests. However, the error was quite consistent for all yaw angles. Since the styrofoam prototype was only tested in the last session and because of the discrepancies, it was decided to only use the results from the last test when evaluating the prototype. At least two more wind tunnel tests were planned to verify the reliability of the results, to test further prototype alteration, and to test the final product. Unfortunately, the wind tunnel broke down the week before Easter, and was not running for the rest of the semester.

Ideally, the car should have been re-mounted and the equipment re-calibrated in between different runs to map errors due to mounting and calibration, which e.g. Mercker described in his blockage correction experiments [13] in 1986. However, this was considered unnecessary use of time considering the limited time available in the wind tunnel and negligible compared to e.g. the errors due to blockage.

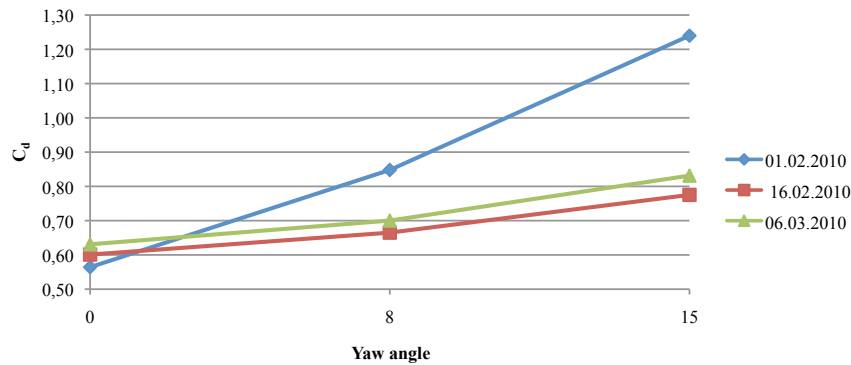


Figure 4.11: A comparison between the drag coefficients of the PureChoice-configuration obtained in the three different wind tunnel tests.

The errors due to mounting and calibration would also been better estimated if the two planned wind tunnel tests had been possible to carry out.

The results from the third wind tunnel test are plotted in figure 4.12, which shows a significant reduction in drag on the prototype model compared to both the PureChoice- and the Fuel Fighter 2009-configuration. The relative improvements are given in table 4.2 and ranges from about 8% at 0° yaw angle to about 15% at 15° yaw angle. Despite the uncertainties in the measurements, this was a satisfying result, bearing in mind the uneven surface and the curvature on the side of the extension which did not match the car design perfectly.

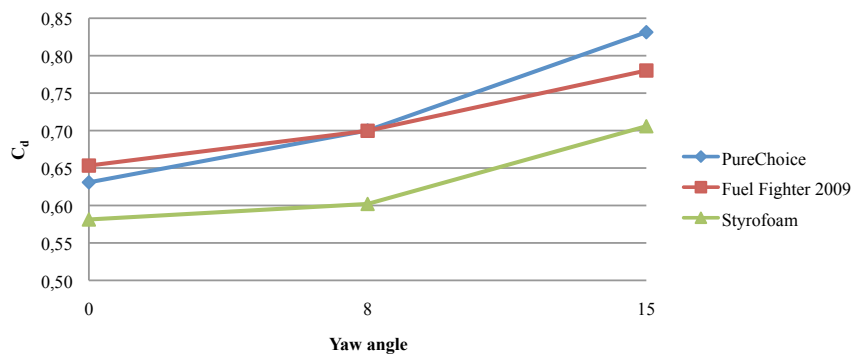


Figure 4.12: The results from the wind tunnel test 06.03.2010 show a significant reduction in drag on the prototype model.

Angle	Styrofoam vs Fuel Fighter 2009	Styrofoam vs PureChoice
0	-7,9%	-11,0%
8	-14,0%	-14,0%
15	-15,1%	-9,5%

Table 4.2: The relative improvement in drag coefficient due to the prototype.

#### 4.7.1 Blockage and $C_d$ -value

The values of the measured drag coefficients were, for several reasons, higher than expected before the wind tunnel tests were performed. First of all, the CFD-calculations executed by the PureChoice-team yielded a  $C_d$ -value of 0,288 [3]. They used a simplified CAD-model of the car without wheels and mirrors, which would certainly have increased the drag somewhat. Second, the Fuel Fighter 2008-team measured the  $C_d A$ -value of the original car to be 0,30, or  $C_d = 0,41$  by using their calculated projected frontal area of 0,74 m<sup>2</sup>. By extending the car using the prototype shown in figure 4.13, they achieved a  $C_d A$ -value of 0,15, equal to  $C_d = 0,20$  [24]. However, when examining their calculations, an error regarding the voltage output to drag force conversion was revealed. They also reported some problems with inconsistent wind tunnel testing results. Last, today's typical production cars have a drag coefficient ranging from about 0,24 up to  $\sim 0,40$  [10]. Based on the above mentioned, it was in this project expected a drag coefficient in the range of 0,30 to 0,40.



Figure 4.13: The prototype extension used in 2009 [24]

Blockage is, based on literature, assumed to be the largest source of error in the wind tunnel testing in this project. As mentioned in section 3.2.1, it is advised to keep the blockage ratio below 5 – 10%. In this case the blockage ratio was about 19%, which, according to figure 3.1, will overestimate the drag coefficient by approximately 30%. To correct for this, the two different methods presented in section 3.2.1 were used, hereafter called continuity correction (eq. (3.2)) and Mercker correction (eq. (3.3)). The calculated corrected values which can be seen

in table 4.1, are applied to the uncorrected prototype test results and plotted in figure 4.14. By using the largest correction factor, the continuity correction, a  $C_d$ -value in the expected range is found: 0,39 for yaw angle  $0^\circ$ . The more advanced Mercker correction gave a somewhat higher result;  $C_d = 0,45$ . Concerning which method is the best, there are almost as many opinions as there are authors. Equation (3.2) is commonly used in industry because of its simplicity, even though more advanced equations such as Mercker's (3.3) are usually considered better [10]. Due to the uncertainties presented above, one should use care when determining absolute values for drag with blockage correction. Based on the proceeding discussion, it would be appropriate to estimate the drag coefficient to be in the region of 0,40 to 0,45. It is worth noting that by subtracting the error as indicated in figure 3.1, the corrected drag will end up in approximately the same region.

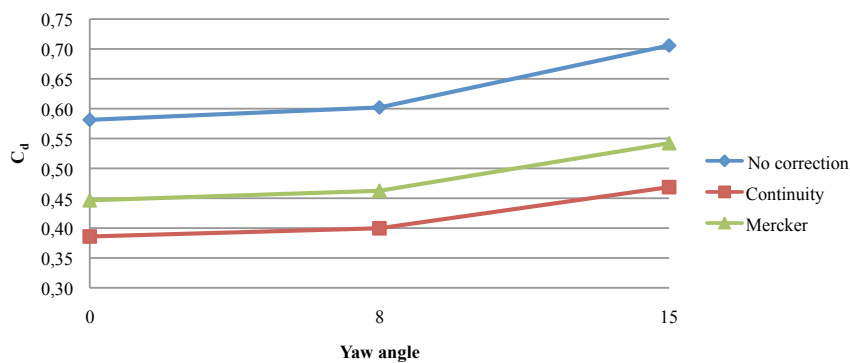


Figure 4.14: The two used blockage correction methods in comparison with the uncorrected results for the styrofoam prototype.

This  $C_d$ -value is somewhat higher than the typical value for today's commercial cars. However, when comparing differently sized vehicles, one should also take into account the  $C_d A$ -value, as discussed in section 2.2. While the projected frontal area of the DNV Fuel Fighter-car is  $0,9 \text{ m}^2$ , the typical frontal area of normal cars are about the double. For instance, the MIRA model, commonly used in many wind tunnel comparison tests, has a frontal area of  $1,856 \text{ m}^2$  [13]. Appendix 1 in ref. [9] gives a list of drag coefficients, frontal area and drag factor ( $C_d A$ ) for a large number of differently sized commercial vehicles. The majority of the vehicles presented has a frontal area of between  $1,7 \text{ m}^2$  and  $2,0 \text{ m}^2$  and hence correspondingly higher  $C_d A$ -value compared to  $C_d$ -value. If one then compares those values to the  $C_d A$ -value for the DNV Fuel Fighter-car, which has a 10% lower  $C_d$ -value than a  $C_d A$ -value, it turns out that the latter experience less aerodynamic drag than most of the vehicles in the reference.

### 4.7.2 Discussion of Error Sources

The ground board was used for two purposes; to elevate the car out of the wind tunnel boundary layer, and in order to measure the forces with the balance. To which extent the elevation of the ground board was sufficient, and to which extent flow disturbance and flow circulation around the ground board affected the results were not prioritized to determine during the wind tunnel sessions. The moving road problem was obviously not examined since no suction or moving belt equipment are available in the wind tunnel at NTNU. The above mentioned effects, combined with blockage errors will certainly affect the validity of the tests compared to the actual drag of the car when driving on a road. However, the purpose of the wind tunnel tests was not primarily to determine an exact value of the drag coefficient  $C_d$ , but to improve the aerodynamic performance of the car. In literature, the *incremental* data are often proven to be quite accurate when evaluating vehicle improvements [10]. A comparison of blockage effects between six European wind tunnels was performed in 1986 by Cooper et al. [22] using scaled truck models, in which concluded with quite large discrepancies in absolute  $C_d$ -values, but much smaller differences in incremental drag. Comparative tests are also extensively used to evaluate and correct blockage corrections [10], where standardized car models such as the MIRA-car [13] and standardized test procedures can be used to compare own results with other tests.

The reliability of the wind tunnel testing was not clarified to the extent wanted, due to the wind tunnel breakdown. Data from more testing would have given the possibility to find an average value of the drag coefficients and use that to find an estimate of the measurement deviance. As mentioned earlier, a 5% deviance between the two measurements that were assumed to be reliable. The deviation is most likely a combination of several error sources. First of all, the calibration of both the balance and the pitot tube introduces uncertainties even though briefly validated as presented in section 4.3.2 and 4.3.3. Second, the mounting of the car on the ground board and the sealing of glitches on the car, e.g. around the door, might have been slightly different from test to test. One third error source can be introduced due to interference of electrical signals. Oscillating signals were observed in the first wind tunnel test, but was stabilized by increasing the sample time in the two last tests.

To ensure that no sudden changes in  $C_d$ -values, primarily due to separation, the results were compared for the three different wind speeds. As can be seen in figure 4.15, represented by the data from the wind tunnel test 06.03.2010, no such effects took place. The slight deviances are considered to be a result of the above mentioned error sources.

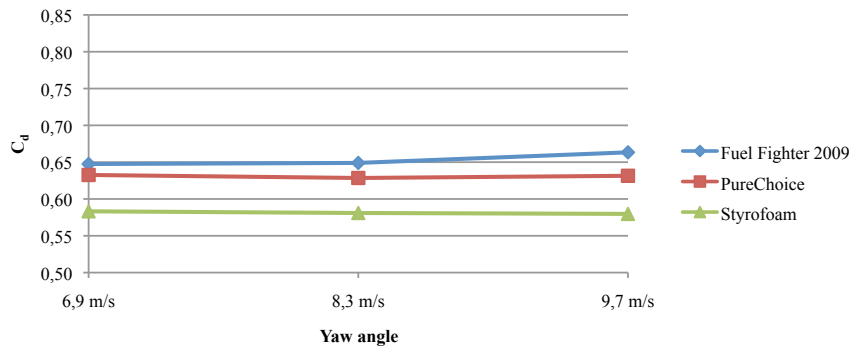


Figure 4.15: No sign of sudden changes in  $C_d$ -values were observed in the operative speed range of the car. The plot is based on results from the wind tunnel test 06.03.2010, at  $0^\circ$  yaw angle.

Despite all uncertainties, the existence of an aerodynamic benefit from the produced end extension is considered well-founded. To let J. Katz [9] summarize the wind tunnel testing:

‘Since vehicle improvement requires only incremental data (to judge if an idea is good), productive vehicle improvements can be achieved with minimum resources (good results have been achieved with 14 per cent blockage in a wind tunnel with no moving ground belt).’ (p. 97)

## 4.8 Computer Aided Design

Computer Aided Design (CAD) was an important part of the production process applied in this project. The application chosen by the team for this purpose was Autodesk<sup>®</sup> Inventor<sup>™</sup>. The authors of this paper had little or no experience in using this kind of software before embarking on the project, and consequently quite a substantial amount of time went into familiarization with Inventor. Complicating matters was the fact that previous teams used different software tools when building 3D models of the entire vehicle. Creating parts to be attached to the existing body of the car involves knowing the exact geometry on to which the parts are to be mounted. In this respect, a practical way of incorporating the existing geometry is to use the same 3D files as originally used when creating the car monocoque. Due to the differing of file formats used, work had to be done converting existing data into a format onto which further modeling work could be performed. Specifically concerning modeling of the new end extension, problems



arose when doing work on an imported file, into which a significant amount of time was spent resolving. Figure 4.16 shows a 3D model of the final production end extension design, along with an exploded 3D view of the entire vehicle and its main components.



Figure 4.16: Exploded view of DNV Fuel Fighter 2010.

## 4.9 Production

### 4.9.1 Production at Kongsberg

From the fall of 2009 the DNV Fuel Fighter team had an oral agreement with Kongsberg that they would, among other things, assist in the production of the carbon fiber parts. However, in early March of 2010 they decided not to fulfill this original agreement and instead provide their entire sponsorship in the form of cash. This had quite a substantial impact on the amount of work resting on the shoulders of the team members, and the time available for various aspects of the project. It basically meant that all carbon fiber parts would have to be

built entirely by the team itself, mostly without any assistance from people with experience in carbon fiber moulding. A lot of trial and error was the result, at which a significant amount of time was spent. The following is a description of the process involved in creating parts in carbon fiber, with emphasis on the specifics around the construction of the rear extension. In section 4.9.5 details on the materials used are briefly discussed.

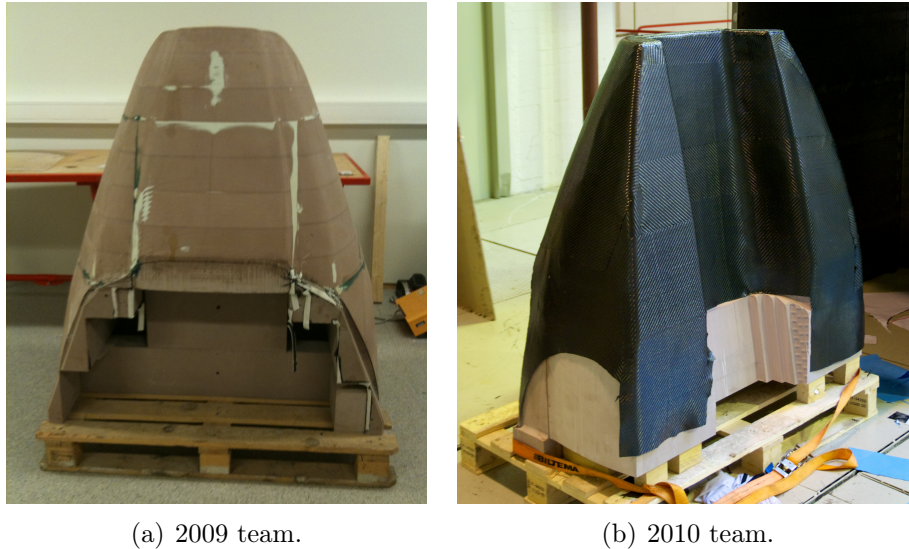
### 4.9.2 Milling of Mould

To create the parts from carbon fiber, every part needs a mould onto which the carbon fiber can be fixed. Since it was decided that the top and side shape of the mould for the end extension would be the same as that of the 2009 team, the intent was to mill the underside of that mould. Problems did however arise with this plan. The mould was too large to fit into any milling machine known to the team at the time, and there existed no saw on NTNU big enough to cut it into smaller pieces. On top of this it turned out the mould was not massive as well as full of screws and bolts. A new mold needed to be created from scratch.

Ebaboard 60-1 is the material the team has chosen for creating moulds for the carbon fiber parts. It can handle the temperatures required for carbon fiber moulding, can be reused and has otherwise good mechanical properties for this purpose. It was delivered in either 100 mm or 50 mm plates at 1500 mm by 500 mm. The mold made by the 2008/2009 team was made out of 100 mm thick pieces of Ebaboard 60-1 that were glued together after being individually machined in a CNC machine. The individual plates and the structure can be seen in figure 4.17(a). This way of building a mould is very labour intensive as the machining process, the work needed to assemble the individual blocks together and eventually creating a smooth surface for the mold is very time consuming. The optimal process would involve creating a slab of Ebaboard the size of the extension, machining the whole mould in one go and finish off with a fairly small amount of work on the surface quality. Thanks to SINTEF Marine represented by Lars Øien this was, for the most part, how the process ended up. Due to heavy work load at SINTEF Marine as well as various unanticipated problems, the mould was delivered roughly one and a half week later than initially estimated, at 28.04.2010.

### 4.9.3 Carbon Fiber Moulding

The casting process used is that of vacuum casting, the procedure of which is briefly discussed in this section.



(a) 2009 team.

(b) 2010 team.

Figure 4.17: End extension moulds.

Once the mould has a mechanically smooth surface, a release film is applied. In this case the release agent used was RenLease QV 5110 which is applied like a wax.

The carbon fiber type used is a prepreg from Advanced Composites Group. Using a pair of scissors one can quite easily cut this material into the desired shape and lay it on the mould. The number of layers and their direction with respect to each other is chosen based on the structural properties needed for the particular product. Specifics on the carbon fiber material is found in section 4.9.5. Once layers of carbon fiber are satisfactory added to the surface of the mould, the next step is to add a layer of peel ply and cloth. The peel ply is a layer of breathing synthetic fabric that has the purpose of easily releasing from the carbon as well as preventing the cloth from sticking. Cloth is added so that the vacuum will disperse evenly over the carbon fiber. The last step before curing the part in an oven at  $80^{\circ}\text{C}$  for 5 hours is to seal it completely airtight using a plastic bag and sealant tape before evacuating the air with a vacuum pump.

#### 4.9.4 Curing Process

Most carbon fiber parts for the car were cured in the large oven located at the Department of Engineering Design and Materials (IPM). That oven, however, was not big enough for the end extension. With help from the Thermal Energy Group

at Department of Energy and Process Engineering a provisional oven was purpose-built for curing the large end extension at the desired temperature of 80°C, as seen in figure 4.18.



Figure 4.18: Provisional oven.

#### 4.9.5 Materials

**Carbon fiber:** The ACG VTM<sup>®</sup>260 prepreg is normally stored in a freezer to delay hardening of the epoxy. Compared to the prepreg used last year it can withstand a significantly longer period of time in room temperature (up to a month), a property that is practical when working with it since it does not become stiff and cumbersome quickly. Details are in the data sheet found in reference [26].

**Epoxy:** The epoxy system used is based on Araldite ESR3, Hardener ESH3 and accelerator ACC 399. All three components are mixed based on their respective weight ratios. Once the components are mixed the hardening process begins with the cure time depending on the amount of, if any, accelerator used. The various cure times can be found in the epoxy datasheet in reference [27].

**Ebboard:** This is the material in which the moulds have been machined. Notable from the datasheet, found in reference [28], are the following properties:

- Fine structure
- High strength values
- Good edge strength
- High heat resistance
- Good resistance against solvent
- Very well workable (contains no abrasive fillers)

**RenLease QV 5110:** A cloth applied wax based release agent for assisting in the release of the carbon fiber from the Ebaboard mould after curing.

#### 4.9.6 Production Problems

During the production of the end extension several problems of varying complexity and severity did arise. Some of these had a direct impact on the quality of the end product and are as such considered relevant for a brief discussion.

Creating vacuum on a mould the size of the end extension is a challenge. At the time of construction three pieces of plastic bag had to be joined together in order to cover the entire mould. It is preferred to use a single large bag as it reduces the likelihood of leakage by removing the joins. The attempt initially was to seal the bag onto the Ebaboard along the base of the mould. Due to small cracks in the mould and the fact that the sealing tape used did not attach to Ebaboard sufficiently, this method did not result in an air tight seal. The solution to this problem was placing a metal plate beneath the whole mould and subsequently sealing the bag onto the smooth metal surface. From figure 4.19 the initial seal onto the Ebaboard and the subsequent metal plate beneath the mould can be seen.

Due to the two Ebaboard pieces being of different lengths after milling, the lower piece had to be raised approximately 8 cm off the floor for it to become flush with the top half. This was done by placing 8 pieces of wood cut in the right length beneath the shortest half. However, in retrospect that solution was not optimal since it creates a large void beneath the half of the mould it is raising. When evacuating the air at the end of the bagging process, the plastic bag will enter into the void until it eventually bursts. The effect of this was an inability to maintain the desired amount of vacuum for the duration of curing. The compromise used was switching the vacuum pump on for a few seconds roughly every 5 minutes in an attempt to have some pressure on the mould. It is worth noting that at the time

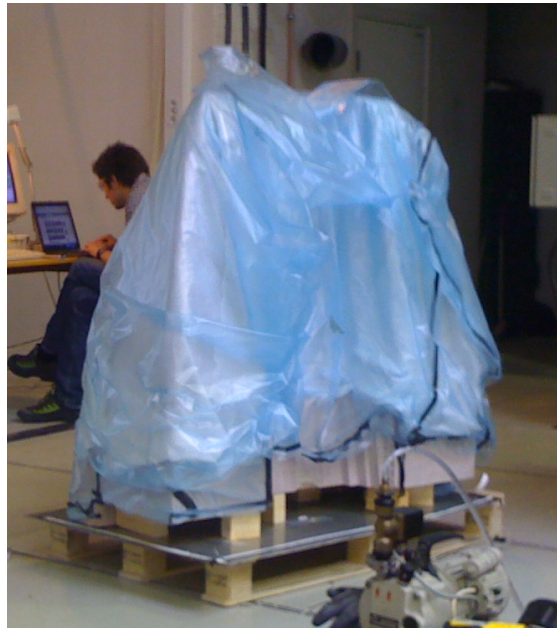


Figure 4.19: Mould with initial bag solution.

of construction the competition was only days away and hence no time to start over. The end result of this curing process was a carbon fiber part that could not carry its own weight. Most likely due to the lack of sufficient vacuum, the epoxy escaped into the cloth and peel ply leaving very little left in the carbon fiber itself for structural integrity. The quick fix was brushing epoxy on the carbon fiber part while it was still in place on the mould. Since no even pressure could be applied to the surface, the carbon fiber was not perfectly attached to the surface of the mould resulting in a part somewhat off in shape compared to intended design.

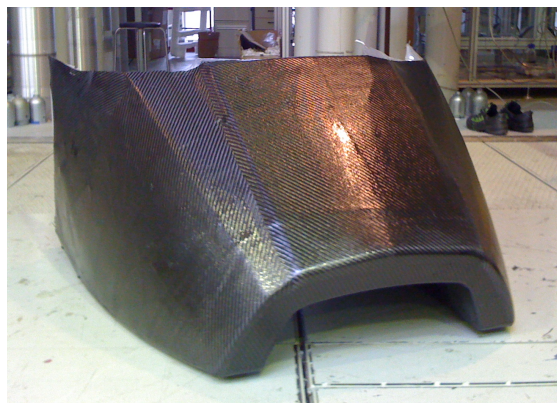


Figure 4.20: Finished casted end extension.



## 4.10 Final Design

Since only one prototype went through testing, the final design for production had to be based entirely on the experience gained by that one test. The results did, as mentioned in section 4.7, show a reduction in drag for the yaw angles of inflow tested. In addition to measuring the drag forces with the prototype end extension in place, measurements of air speed were manually performed using a hand held pitot tube. Measurements were taken at four locations at the rear of the car, as indicated in figure 4.21 and described in table 4.10.

1	7,5 m/s	Top side, at the onset of the end extension
2	6,7 m/s	Top side, about 10 cm upwind of the extension edge
3	3,7 m/s	Bottom side, about 10 cm upwind of the extension edge
4	7,7 m/s	Bottom side, at the onset of the end extension
N/A	7,9 m/s	Freestream

Table 4.3: Measured velocities along car body.

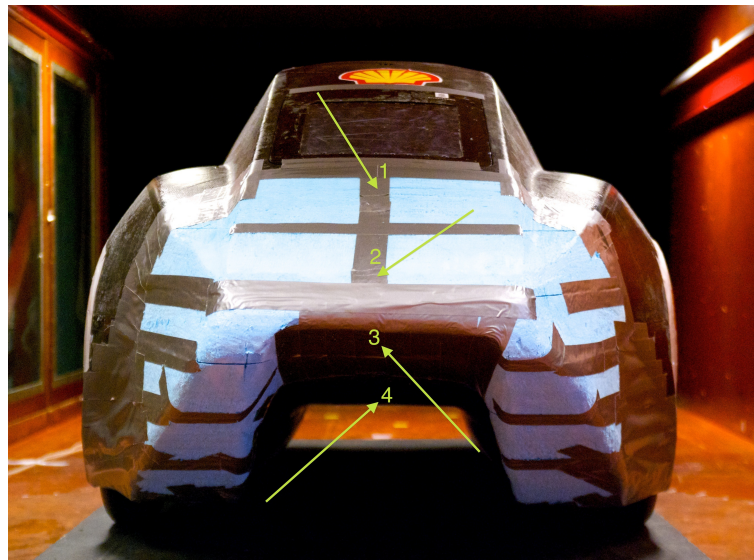


Figure 4.21: Points of velocity measurements along vehicle body.

The measurements were taken by hand at about 5 cm distance from the surface. Even though they are very approximate, they do indicate that something happens in the aft part of the tunnel on this design. The height of the side walls of the prototype tunnel shape did rather rapidly decrease, possibly resulting in extensive leakage of air below out to the sides. Since the pressure regime is not known in

that region, it is difficult to speculate whether or not leakage of this kind would be plausible. If, however, this is the case, then based on continuity it could be part of the reason why such a drastic reduction of flow speed is seen in the tunnel as opposed to on the top surface. In addition to this it is possible that the flow separated from the roof of the tunnel. Visualizing this conclusively however, proved difficult using wool tufts. It is preferable to have both airstreams over and under the car join in as similar states as possible to minimize the energy lost to the wake. Due to these observations, and the inability to perform further testing in depth, it was chosen to both change the inclination of the tunnel from approximately  $12^\circ$  to  $8^\circ$  and to increase the height of the tunnel at the rearmost part of the end extension. The reduction in tunnel inclination provides means for the flow to more easily remain attached.

As briefly mentioned in section 2.1, the profile of the trailing edge may influence the drag of the vehicle. On the final end extension design the trailing edges were rounded with a radius of 2 cm. It is not known whether or not this is optimal. However, it was chosen as a compromise between a sharp edge, that might give lower drag, and a large radius rounded edge, that would be consistent with the look of the car.



# Chapter 5

## Conclusion

### 5.1 Notes on Shell Eco-marathon 2010

In place at Euro Speedway Lausitz the vehicle was not tested, and various assembly work remained. The effect of bringing an incomplete vehicle to Germany was the inability to do final adjustments to the electronic control system in relationship to fuel cell and motor. Hence, when the control system failed, there was not enough time to troubleshoot and debug, resulting in failure to complete an approved run of seven laps. This is considered nothing more than a testament to the importance of planning and respect for deadlines, but the result was nonetheless unfortunate.

Had there been a greater emphasis in the competition on realism with respect to speed and road safety, the aerodynamic aspect of Shell Eco-marathon would be significantly more interesting and challenging. This would, among other things, impose a need for research into the cross-wind stability and lift forces on the vehicle to maintain a steady path.

### 5.2 Conclusion

With respect to development of the end extension, prototype testing gave very satisfying results. Unfortunately, the final version of the extension could not be tested due to the wind tunnel breakdown. However, in the authors' subjective opinion, the new extension is most likely to give at least the same improvement as for the prototype due to more streamlined shape and better surface. If further development on the existing vehicle is desired, conclusive wind tunnel tests should



Figure 5.1: DNV Fuel Fighter 2010.

be performed on the final 2010 end extension design. It is recommended that emphasis in this respect is given to ensuring that flow separation is avoided on the end extension underside.

A thorough evaluation of how the fuel cell can be supplied sufficiently with air whilst minimizing energy consumption should be conducted. Especially into whether a system based on flow driven by naturally occurring or artificially created pressure differences, will consume the least amount of energy. The same applies to driver ventilation, and in this respect it is highly recommended that the results of Eco-marathon Driver Performance [20] be carefully evaluated.

Due to the nature of the project as conducted this year, a relatively short amount of time was available for the actual development of new aerodynamic features. The initial familiarization with road vehicle aerodynamics via literature, the amount of time required for production of various components, and all other time consuming administrative tasks, result in a somewhat cramped development process. It is recommended that future teams focus on aerodynamics from the very beginning. This will allow for thorough research with both CFD and prototypes, as well as testing and verification of final produced solutions.

# Bibliography

- [1] Shell. History of Shell Eco-marathon;. Available from: <http://www.shell.com/home/content/ecomarathon/about/history/> [cited 20.05.2010].
- [2] Shell. Current Records;. Available from: [http://www.shell.com/home/content/ecomarathon/about/current\\_records/](http://www.shell.com/home/content/ecomarathon/about/current_records/) [cited 20.05.2010].
- [3] Bjugstad LI, Grudic E, Hembre B, Henriksen M, Herland O, Jahren E, et al. PureChoice - 0,012 liter på mila [Fall Project]. NTNU; 2008.
- [4] Pettersen B, Christensen S, Lund Ø, Ebbesen M, Gellein A. 1000 km/l i Shell Eco-marathon 2009! [Fall Project]. NTNU; 2008.
- [5] Shell. European Rules Shell Eco-marathon 2010;. Available from: [http://www.shell.com/home/content/ecomarathon/europe/for\\_participants/european\\_rules/](http://www.shell.com/home/content/ecomarathon/europe/for_participants/european_rules/) [cited 12.06.2010].
- [6] Santin JJ, Onder CH, Bernard J, Isler D, Kobler P, Kolb F, et al. The World's Most Fuel Efficient Vehicle: Design and Development of Pac-car II. Verlag der Fachvereine Hochschulverlag AG an der ETH Zurich; 2007.
- [7] ETH;. Available from: [http://www.paccar.ethz.ch/pictures/pac\\_car\\_II\\_miscellaneous/messe\\_zuerich?hires](http://www.paccar.ethz.ch/pictures/pac_car_II_miscellaneous/messe_zuerich?hires) [cited 12.06.2010].
- [8] Carr GW. Scope and means for drag reduction in cars and commercial vehicles. In: Vehicle Aerodynamics. Short Course 1984-01. von Karman Institute. Rhode Saint Genese Belgium; 1984. .
- [9] Katz J. Race Car Aerodynamics: Designing for Speed. 2nd ed. Bentley Publishers; 2006.
- [10] Barnard RH. Road Vehicle Aerodynamic Design. 2nd ed. MechAero; 2001.
- [11] Mcbeath S. Competition Car Aerodynamics. Haynes; 2006.

- [12] Versteeg HK, Malalasekera W. An Introduction to Computational Fluid Dynamics - The Finite Volume Method. 2nd ed. Pearson Education Limited; 2007.
- [13] Mercker E. A blockage correction for automotive testing in a wind tunnel with closed test section. *Journal of Wind Engineering and Industrial Aerodynamics*. 1986;22:149–167.
- [14] Glauert H. Wind tunnel interference on wings, bodies, and airscrews. No. 1566 in Reports and Memoranda. Aeronautical Research Council (ARC); 1933.
- [15] Maskell E. A theory of the blockage effects on bluff bodies and stalled wings in a closed wind tunnel. No. 3400 in Reports and Memoranda. Aeronautical Research Council (ARC); 1961.
- [16] Kramer C. Introduction Into Vehicle Aerodynamics. In: *Vehicle Aerodynamics*. Short Course 1984-01. von Karman Institute. Rhode Saint Genese Belgium; 1984. .
- [17] Wuest W. Verdrängungskorrekturen für rechteckige Windkanäle bei verschiedenen Strahlbegrenzungen und bei exzentrischer Lage des Modells. *Z Flugwiss*. 1961;9:15–19 and 362.
- [18] Volvo. New state-of-the-art wind tunnel gives Volvo buyers reduced CO2-emissions and lower fuel consumption;. Available from: <http://www.volvocars.com/my/top/about/news-events/pages/default.aspx?itemid=17> [cited 26.05.2010].
- [19] Burgin K, Adey P, Beatham J. Wind tunnel tests on road vehicle models using a moving belt simulation of ground effect. *Journal of Wind Engineering and Industrial Aerodynamics*. 1986;22(2-3):227–236.
- [20] Tveito KO, Eide JTW, Vallee ECY, Sivertsen SS, Rosvoldaunet AS. Eco-marathon Driver Performance. Norwegian University of Science and Technology; 2009.
- [21] Tavoularis S. *Measurement in Fluid Mechanics*. Cambridge University Press; 2005.
- [22] Cooper K, Gerhardt H, Whitbread R, Garry K, Carr G. A comparison of aerodynamic drag measurements on model trucks in closed-jet and open-jet wind tunnels. *Journal of Wind Engineering and Industrial Aerodynamics*. 1986;22(2-3):299–316.
- [23] Voigt U. Lausitzwetter; [cited 11.06.2010]. Available from: <http://www.lausitzwetter.de/>.

- [24] Storaker A, Pettersen BS, Christensen S, Skogen DV, Birkeland ØF, Ebbesen MC. The World's Most Fuel Efficient Car [Master's thesis]. NTNU; 2009.
- [25] Milliken WF, Milliken DL. Race Car Vehicle Dynamics. SAE International; 1995.
- [26] Advanced Composites Group. Datasheet ACG VTM®260;. Available from: [http://www.advanced-composites.co.uk/data\\_catalogue/catalogue%20files/pds/PDS1154-VTM260-issue7.pdf](http://www.advanced-composites.co.uk/data_catalogue/catalogue%20files/pds/PDS1154-VTM260-issue7.pdf) [cited 24.05.2010].
- [27] Lindberg and Lund AS. Datasheet Araldite ESR3/Hardener ESH3 + ACC 399;. Available from: <http://www.lindberg-lund.no/files/Tekniske%20datablade/VAN-ESR3-TD.pdf> [cited 24.05.2010].
- [28] Ebalta. Datasheet Ebaboard 60-1;. Available from: [http://www.ebalta.co.uk/products/product\\_datasheets/ebaboard/modelling\\_boards/datasheet\\_uk\\_ebaboard\\_60-1.pdf](http://www.ebalta.co.uk/products/product_datasheets/ebaboard/modelling_boards/datasheet_uk_ebaboard_60-1.pdf) [cited 24.05.2010].